الجمهورية الجزائرية الديمقراطية الشعبية

PEOPLE'S DEMOCRATIC REPUBLIC OF ALGERIA

وزارة التعليم العالي والبحث العلمي

Ministry of Higher Education and Scientific Research

Aboubakr Belkaïd University

Tlemcen

Faculty of TECHNOLOGY

THESIS

Presented to acquire a **MASTER'S DEGREE**

In: CIVIL ENGINEERING

Speciality: STRUCTURAL ENGINEERING

By: CHIMOTO TAWANDA TINASHE and MARADZIKA FARAI KELVIN

Title:

EARLY AGE BEHAVIOUR OF CONCRETE IN MASSIVE STRUCTURES.

Defended on the 6th of July 2021, before a jury composed of:

Dr ROUISSAT Bouchrit	Associate Professor	University of Tlemcen	President
Dr SMAIL Nadia	Associate Professor	University of Tlemcen	Examiner
Pr MATALLAH Mohammed	Professor	University of Tlemcen	Supervisor
Mr TAIBI Abdelsemi	Phd Student	University of Tlemcen	Co-supervisor

Acknowledgements

By the grace of our omnipresent Lord, this Master's thesis work concludes an amazing and yet worthwhile journey, at University of Tlemcen. This work was done with funding and support from University of Tlemcen's Department of Civil Engineering, from March 2021-June 2021.

We would like to express our utmost gratitude to our thesis supervisor and advisor, Pr M Matallah for his unwavering support throughout the entire journey. Strict and a sucker for excellence but executes his duties with grace and panache. Equally gifted was his co-supervisor, Mr A Taibi, a man so fluent in the language of humility and hard work who went an extra mile to ensure that our work lacked not of quality. Their constant counsel and encouragement were the energy which kept us going up and forward. We acknowledge the entire crew at the RISAM Research Laboratory for creating a warm working ambiance. Their invaluable understanding and experience enabled us to conduct our numerical simulations timely.

We extend our unmeasurable gratitude to Dr B Rouissat and Dr N Smail for agreeing to form a jury for this work regardless of their busy schedules.

Our thanks also go to all our teachers over the years of study. They are pillars of the knowledge we stand on.

Appreciated also, is the camaraderie love and kindness shared by our classmates and fellow students at the department. Comrades, rubbing shoulders with you was as beautiful and fulfilling as it gets.

Finally, our hearts are full, courtesy of everyone who participated directly or indirectly the completion of this work. Some of you inspired us silently as you were motoring your various assignments with such aplomb.

Dedication

I dedicate this work to my parents BENONE ZVIKOMBORERO and FUNGAI BENONIA CHIMOTO for all the love and unwavering support they have given me to be where I am today. I also want to thank my siblings and the whole Chimoto and Mapako families for always being there for me and keeping me in their prayers.

TAWANDA TINASHE CHIMOTO

Dedication

This Thesis is dedicated to you my parents, FANNWELL and CLARAH MARADZIKA, remarkable and quintessential specimens both. The litany of prayers you sent high up for me here manifested. That I did this work in honour of you, is the stuff of dreams an ordinary boy grew up envisaging. It's the little I could do to try and match your undiminishing compassion, prudence and unconditional love.

FARAI KELVIN MARADZIKA

Abstract

Throughout construction, the internal rise of temperature due to the heat released by cement hydration and its interaction with the ambient environment often results in significant volumetric deformations. When restrained either internally or externally, these deformations may lead to the development of considerable tensile stresses and, consequently, to the cracking of concrete. Whenever such stresses attain the concrete tensile strength, cracking occurs, which may in turn impair the functionality, serviceability and durability of the structure. In massive concrete structures internal restraining conditions are often prevalent, such as in thick blocks, armour units, footings and dams. For this reason, establishment of temperature control measures is frequently deemed a necessity as natural cooling is often found short. In this work, the question around the early age concrete problem will be addressed, together with methods of limiting its effects.

Reducing thermal cracking in a restrained massive concrete structure can be done by lowering or controlling the temperature rise. Several methods of cooling can be used to achieve this. These methods may be divided into pre-cooling and post-cooling methods. There has been quite a handful of papers and literature addressing this hydration problem and ways to control it using the macroscopic scale, a little to nothing has been published using the mesoscopic scale. To overcome this drawback, the present work proposes ways to simulate the pre-cooling and post-cooling effect using the mesoscopic scale. The proposed approach is also used to predict the thermomechanical behaviour of random real specimens.

Key words: mesoscopic modelling, early age concrete, hydration, damage, cracking.

Résume

Durant la construction des structures massives, l'élévation de température interne due à la chaleur dégagée par l'hydratation du ciment et son interaction avec le milieu ambiant se traduit souvent par des déformations volumétriques importantes. Lorsqu'elles sont contraintes intérieurement ou extérieurement, ces déformations peuvent conduire au développement des autocontraintes de traction importantes, et par conséquent, des micros fissures sont apparaitre directement après la construction.

Dans les structures béton en grande masse, les conditions de retenue internes sont souvent répandues, comme dans les blocs épais, les unités de blindage, les semelles et les barrages. Pour cette raison, la mise en place de mesures de contrôle de la température est souvent considérée comme une nécessité car le refroidissement naturel est souvent insuffisant. Dans ce travail, la problématique du comportement de béton au jeune âge sera abordée, ainsi que les méthodes pour en limiter les dommages induits au béton a l'âge précoce.

La réduction de la fissuration thermique dans une structure en béton massif retenu peut être réalisée en abaissant ou en contrôlant l'élévation de température. Plusieurs méthodes de refroidissement peuvent être utilisées pour y parvenir. Ces méthodes peuvent être divisées en méthodes de pré-refroidissement et de post-refroidissement. Il y a eu pas mal d'articles et de littérature traitant de ce problème d'hydratation et des moyens de le contrôler à l'aide de l'échelle macroscopique, un peu ou rien n'a été publié à l'aide de l'échelle mésoscopique. Pour surmonter cet inconvénient. Le présent travail propose des moyens de simuler l'effet de pré-refroidissement et de post-refroidissement à l'aide de l'échelle mésoscopique. L'approche proposée est également utilisée pour prédire le comportement thermomécanique d'échantillons réels aléatoires.

Mots clés : modélisation mésoscopique, béton jeune âge, hydratation, endommagement, fissuration.

ملخـــص

اثناء انجاز مشاريع الكبرى ، غالبًا ما يؤدي ارتفاع درجة الحرارة الداخلية بسبب الحرارة المنبعثة من التفاعل الداخلي لإسمنت. كذلك تفاعل مع البيئة المحيطة إلى حدوث تشوهات حجمية كبيرة. عندما يتم إجهادهم داخليًا أو خارجيًا ، يمكن أن تؤدي هذه التشوهات إلى تطوير ضغوط ذاتية شد ، وبالتالي ، تظهر الشقوق الدقيقة مباشرة بعد البناء. في الهياكل الخرسانية السائبة ، غالبًا ما تكون ظروف التقييد الداخلية سائدة ، كما هو الحال في الكتل السميكة والوحدات المدرعة والقواعد والسدود. لهذا السبب، غالبًا ما يُنظر إلى تنفيذ تدابير لتحكم في درجة الحرارة لأن التبريد الطبيعي غالبًا ما يكون غير كافٍ. في هذا العمل، ستتم معالجة مشكلة سلوك الخرسانة في سن مبكرة، بالإضافة إلى طرق الحد من الضرر الناجم عن الخرسانة في سن المبكرة. يمكن الحد من التشقق الحراري في هيكل خرساني صلب محتفظ به عن طريق خفض أو التحكم في ارتفاع درجة الحرارة. هناك عدة طرق تبريد التي هدفها تقليص درجة الحرارة في الخرسانة. كان هناك عدد غير قليل من المقالات العلمية التي تتناول مشكلة التفاعل الداخلي لإسمنت في انجاز مشاريع الكبرى وطرق التحكم في سلوك الخرسانة في هدا العمل. قمنا بمحاكاة رقميه و بالتقنية ميكروسكوبيه وكذلك بدراسة تأثير و التبريد المسبق وما بعد التبريد للتنبؤ بالسلوك الحراري الميكانيكي الخرسانة في السن المبكرة.

الكلمات المفتاحية السن المبكرة لخرسانة ،محاكاة ميكروسكوبيه. التفاعل الداخلي لإسمنت، تشوهات، تصدعات.

Table of Contents

List of Figures.

List of Tables.

Abbreviations.

w/c: Water to Cement ratio

a/c: Aggregate to Cement ratio

QXRA : Quantitative X-Ray Diffraction Analysis

CTE: Coefficient of Thermal Expansion

DCS: Degree of Capillary Saturation

RCC: Rolled Compacted Concrete

ITZ: Interfacial Transition Zone

EA: Early Age

WEA: Without Early Age

General Introduction

Concrete which is also known as the man-made rock in academia and in the scientific world, is the leading and mostly used material in the built environment. All this is courtesy of its raw materials being readily available, its workability, durability and its significant resistance to corrosion and alien attacks such as fire, frost amongst others. Concrete is a heterogeneous material formed by a series of chemical reactions between raw materials. The constituents normally include a binder (cement), water, sand, coarse aggregate and admixtures.

The go to material when building large structures, including, but not limited to, hydropower plants and dams has always been concrete as they are expected at the bare minimum to be resilient and thus require high durability. Humongous amounts of concrete are needed to birth such structures, and we are left with imperative heat generation during the cement hydration. The eventual hydration provokes a temperature rise in the structure and with unfashionable help from restrained edges, may cause thermal related cracks which affect the integrity and safety of the structure. The effects are more severe in extreme weather conditions. For structures which are exposed to water pressure such as hydropower plants, thermal cracking may cause leakages and reinforcement corrosion. In the case of nuclear reactors, the cracks are equally life threatening as they can cause explosions and everything undesirable about radioactive radiation.

To mitigate and counter this elephant in the room, a lot of countries have adopted use of type I Portland cement, its ingenuity is allied to its low heat generation during hydration. As such, it is often used for hydropower plant and dam constructions. Unfortunately, its use can only go this far and is not sufficient to prevent cracks and thermal damages in massive structures. This special cement works best in union with other measures to reduce the heat generation or to control the temperature rise due to the hydration heat.

In a bid to lower the risk of thermal cracking the concrete temperature has to be reduced. Several methods can be applied to reduce the temperature in massive concrete structure. Those methods can be sub-divided into pre-cooling and post-cooling methods. Pre-cooling methods are based on reducing the amount of heat generated by cement with substituting materials or by lowering the concrete temperature at casting. Post-cooling methods are used to lower the temperature of the concrete body during hydration.

Objectives

The brains behind this master project were moved by the need to identify and evaluate the different methods available with the hope of limiting and controlling the temperature rise and or fluctuations during hydration within massive concrete structures. The blueprint would identify, if any, the potential for reducing heat generation and crack risk during hydration for different types of methods and find alternatives to conventional cooling pipes. Part of the study will scrutinize concrete dimensions' effect on the maximum hydration temperature.

Work Structure

This work has four parts:

The first chapter is dedicated to a bibliographical study on the early age behaviour of concrete, centred on the hydration problem in young concrete and the resultant types of deformations.

In the second chapter we have a brief discussion on the various methods employed in today's industry in trying to combat or minimise the early age hydration problem in massive concrete structures.

The third chapter is dedicated to modelling and analysis of the early age effect of hydration on concrete. This section also looks at the effect of dimensions on the hydration temperature evolution in concrete.

The fourth chapter is devoted to the evaluation of the two main cooling methods which are aggregate cooling and pipe cooling. It goes on to evaluate the effect of different granular classes using aggregate cooling.

Chapter 1: The Effect of Early Age Concrete Behavior in Massive Structures.

1.1 Introduction.

The knowledge of the behavior of concrete at early age has proven to be very useful over the past decades. With the evolution of construction and an increased tendency in the construction industry to build bigger, comprehension of the problems associated with mass concrete at early age is now a must. In this section we will look into the primary problems associated with early age concrete.

1.2 Definition of a massive concrete structure.

A massive concrete structure is a bulky structure with large dimensions that require enormous amounts of concrete during casting. These prompt for measures be taken in combating the heat generated from hydration of cement and the resultant volume changes to minimise cracking. Such structures would include and are not limited to gravity dams, arc dams, mass building foundations, etc. See Figure 1-1

Figure 1-1 Kariba Dam (Zimbabwe). (Muguti et al., 2015)

This definition however, is silent and not inclusive of certain critical structures which are not necessarily massive structures with respect to volumes of concrete used but are massive structures due to their functionally and vulnerability, see Figure 1-2. Smaller structures where internally developed thermal stresses and potential cracks cannot be tolerated are classified as massive structures, for example nuclear power plants / reactors.

Figure 1-2 Qinshan Nuclear Power Plant (China)

1.3 Early age thermal problem in massive concrete structures.

The origins of the concrete thermal problem in massive structures can all be traced to the exothermic reactions during hydration of cement and pozzolans in concrete mixing. This problem is more apparent with the increase in volume of the concrete as the heat released is directly proportional to the volume of concrete.

The heat generated during the hardening of mass concrete produces steep temperature gradients between the concrete and its immediate environment, cognizant of the fact that the concrete surface temperature is lower due to heat dissipation into the environment.

These temperature variations create volumetric changes in concrete (contraction and expansion). When these volumetric changes are restrained by supports and the more mature interior concrete, tensile stresses are formed on the surface of the concrete, and if the tensile stresses become higher than the overall tensile strength of the concrete, cracks begin to form.

1.4 Hydration reaction in concrete.

The hydration reaction of cement is a combination of several exothermic chemical reactions. In addition, these reactions are thermo-activated. In a massive structure at early age, the geometry, the thermal properties of the material, the boundary conditions of the structure and the progress of the hydration of the cement all contribute to an increase in temperature at the heart of the concrete. This rise in temperature in the concrete has mechanical consequences on the behaviour of the structure.

Even limited to Portland cement, the hydration of cement is complex (Hilaire, 2014).We have such a conundrum because Portland cement is made up of many constituents that react when brought in contact with water. Cement is generally considered to be an anhydrous material which reacts with water. The hydration reaction can be observed globally even though it is known that the reaction of cement with water is in fact made up of multiple reactions. Some of the main reaction equations are given below:

- Portland clinker which consists of calcium silicates (alite = C_3S ,and belite = C_2S in conventional cement):

  - $$C_3S + (y + 1.35)H \rightarrow C_{1.65}SH_y + 1.35CH + Q_{C_3S} \quad (1.1)$$
  - $$C_2S + (y + 0.35)H \rightarrow C_{1.65}SH_y + 0.35CH + Q_{C_2S} \quad (1.2)$$

- The remaining part containing C_3A (tricalcium aluminate) and C_4AF (tricalcium aluminoferrite). Gypsum is introduced to regulate the setting:

  - $$C_3A + gypsum + xH \rightarrow (C_6AS_3H_{32}, C_3AH_6, C_4ASH_{12}) + Q_{C_3A} \quad (1.3)$$
  - $$C_4AF + gypsum + xH \rightarrow (AF_m, AF_t, C(AF)H) + Q_{C_4AF} \quad (1.4)$$

with (Q_{C_3A}, Q_{C_4AF}, Q_{C_2S}, Q_{C_3S}) representing the heat released by each elementary reaction.(Briffaut, 2010)

More simply, by considering the reaction of cement with water as a whole, the hydration reaction can be written in the following form:

$$anhydrous\,cement + nH \rightarrow hydrates + Q \quad (1.5)$$

Where Q represent the global heat release in the hydration reaction and H representing water. Figure 1-3 shows the evolution of hydration heat over time.

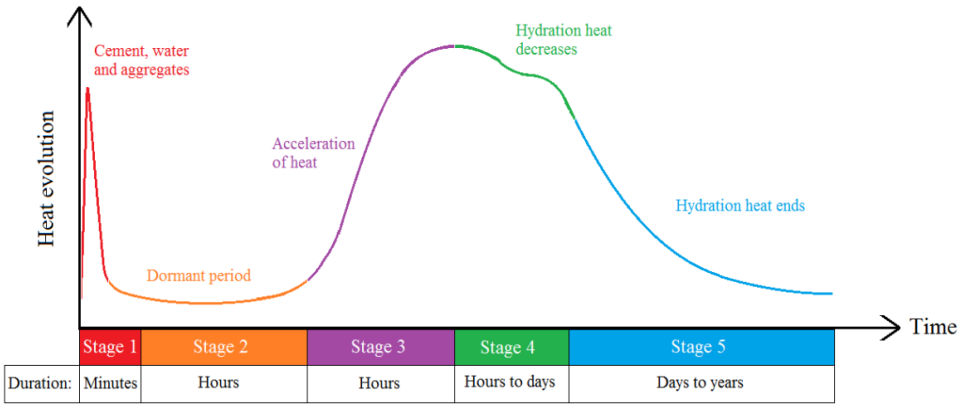

Figure 1-3 Representation of the calorimetric curve of the overall hydration of the cement. (Lagundžija & Thiam, 2017)

1.5 Degree of hydration.

The progress of the hydration reaction is described by the degree of hydration (ξ), characterizing the evolution of the hydration reaction and the evolution of materials over time (from the fluid phase to a solid phase). It can be defined as the ratio between the mass of cement having reacted at time (t) and the mass of anhydrous cement at the origin. It is defined according to the following relation:

$$\xi(t) = \frac{m_h^c(t)}{m_a^c(t=0)} = 1 - \frac{m_a^c(t)}{m_a^c(t=0)} \tag{1.6}$$

Where m_h^c is the mass of hydrated cement, m_a^c is the mass of anhydrous cement. The evolution of the degree of hydration is particularly important because it is directly linked to the evolution of the temperature field of the structure and to the mechanical properties of concrete.

As with the degree of completion, the degree of hydration reaches its maximum value when one of the reagents (water in this instance) is completely consumed. The final degree of hydration is therefore dependent on the w/c ratio. Thus, according to (Powers & Brownyard, 1946), a cement paste cannot be completely hydrated if its w/c ratio is less than 0.418. However, the definition of the degree of hydration differs from that of the degree of completion because in the final state, the degree of hydration is not necessarily equal to one even if the water is present in sufficient quantities. Thus, this theoretical ratio (w/c = 0.418) is not sufficient for the hydration to be complete. This is due to the presence of a layer of hydrates forming around the anhydrous grains and preventing them from reacting with water completely. With that being said, several theories have been brought up which can help in the prediction of the final degree of hydration, (Mills, 1966) proposed the following phenomenological relation to calculate the final degree of hydration :

$$\xi_\infty = \frac{1.031 \times \frac{w}{c}}{0.194 + \frac{w}{c}} \tag{1.7}$$

(Waller, 1999) cited that Mills' relation underestimated the final degree of hydration and proposed the following relation in the absence of any pozzolans :(Hilaire, 2014)

$$\xi_\infty = 1 - e^{-3.3\frac{w}{c}} \tag{1.8}$$

Tests to measure the degree of hydration by Loss on ignition were carried out by Briffaut, seven days after the manufacture of the concrete, the degree of hydration was found to be

up to 0.9 (Briffaut, 2010), see Figure 1-4. In the context of hydration under controlled environmental conditions, the final degree of hydration can be estimated to be in the range of: $0.8 < \xi_\infty < 0.9$ using Briffaut's findings. Due to contradicting estimative methods for the calculation of the final degree of hydration, further research is recommended to peruse this subject decisively.

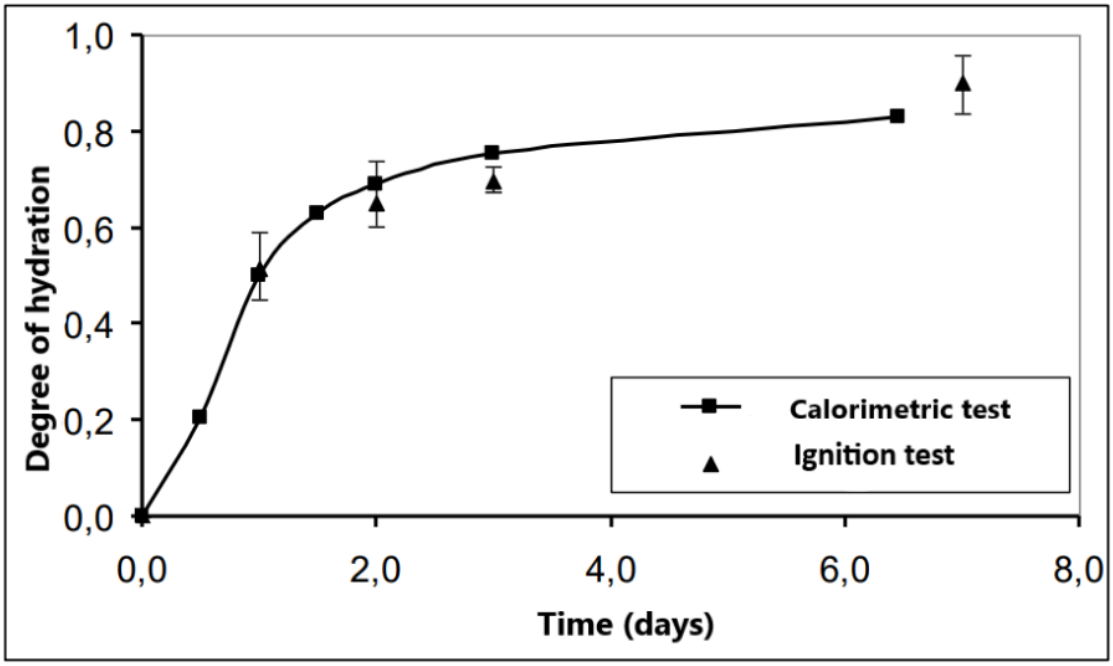

Figure 1-4 Final degree of hydration of CEM I over time. (Briffaut, 2010)

However, the hydration properties of concrete do not only depend on its composition and the properties of its associated cement. Environmental conditions also influence its hydration. The curing temperature is exceedingly not without influence on the hydration process. However, its influence on the final degree of hydration is almost negligible for temperatures less than $60^{\circ}C$.(Hilaire, 2014)

Ambient relative humidity can influence the hydration reaction. Indeed, when the internal relative humidity is below a certain threshold, hydration is stopped completely (Jensen et al., 1999). This observation is important for concrete with a low w/c ratio due to self-drying. While concrete with fairly high w/c ratio is not sensitive to this problem of free water consumption by chemical reactions, the internal relative humidity of this concrete is sensitive to desiccation (to be explained in the following subchapters). However, this process is very slow and due to the massive geometry of the structures studied, only a very small volume of the structure will see its final degree of hydration limited by desiccation.

To conclude, the final degree of hydration of concrete in the case of a massive structure can be estimated simply using a relation like that proposed by (Waller, 1999) (with open recommendations for improvements). The influence of parameters such as curing

temperature or ambient relative humidity do not seem to be significant enough to be taken into account.

1.6 Exothermic and thermo-activation of the hydration reaction.

The degree of hydration and temperature are closely linked. On one hand, chemical reactions are the source of heat releases which lead to an increase in temperature in the structure and on the other hand, the kinetics of these reactions are thermo-activated. The specific heat of the main constituents of concrete are presented in Table 1-1 (Hilaire, 2014) which were condensed from several publications to come up with one figure.

Table 1-1 Specific heat of hydration of the various constituents of concrete (Briffaut, 2010)

Constituant	% **Heat of hydration**
C_3S or alite	510
C_2S or belite	260
C_3A or tricalcium aluminate	1100
C_4AF or tricalcium aluminoferrite	410

Therefore, one way to know the progress of the hydration reaction is to measure the heat given off by this reaction. For cement pastes, it has been shown that the amount of heat released by the hydration reaction is proportional to the degree of hydration estimated by Quantitative X-Ray Diffraction Analysis (QXRA) Figure 1-5. (Hilaire, 2014)

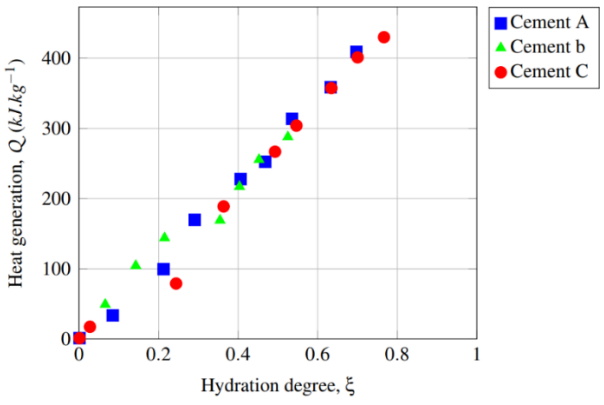

Figure 1-5 Amount of specific heat generated by hydration with relation to the degree of hydration. (Hilaire, 2014)

The progress speed (t) of the hydration reaction increases if the curing temperature is high. The thermal heat released $\dot{Q}$ by the reaction is therefore temperature dependent. This observation can be taken into account via the concept of activation energy introduced by (Arrhenius, 1916). The rate of the degree of hydration $\dot{\xi}$ of the reaction is then dependent on the temperature according to the following relationship:

$$\dot{\xi}(T) = \dot{\xi}(T = T_0).e^{-\frac{E_a^{hyd}}{R}(\frac{1}{T_0}-\frac{1}{T})} \tag{1.9}$$

Where E_a^{hyd} is the apparent activation energy of the hydration reaction and T_0 a reference temperature. The rate of hydration is not only dependent on temperature. The hydration process involves a layer of hydrates forming around the anhydrous grains as discussed earlier on, as a result, the rate of hydration decreases. The kinetics of hydration is therefore related to the progress of the chemical reaction. (Ulm & Coussy, 1995) translate this observation by the introduction of a chemical affinity A, dependent on the degree of hydration in the calculation of the kinetics of hydration:

$$\dot{\xi}(\xi, T) = A(\xi).\exp(-\frac{E_a^{hyd}}{RT}) \tag{1.10}$$

Ultimately, the knowledge of the rate of progress of the hydration reaction can be calculated from equation (1.10). This modelling reveals two parameters, the chemical affinity A and the apparent activation energy E_a^{hyd}.

Table 1-2 Summary of final degree of hydration ξ_∞ of concrete, calculated and experimental.

Author	Method
(Mills, 1966)	$\xi_\infty = \frac{1.031 \times \frac{w}{c}}{0.194 + \frac{w}{c}}$
(Waller, 1999)	$\xi_\infty = 1 - e^{-3.3\frac{w}{c}}$
(Briffaut, 2010)	$Experimental \approx 0.9$
(Ulm & Coussy, 1995)	$\dot{\xi}(\xi, T) = A(\xi).\exp(-\frac{E_a^{hyd}}{RT})$

1.7 Shrinkage.

Concrete can exhibit time dependent deformations in the absence of any applied external mechanical loading. This behaviour, properly termed shrinkage, is defined as a decrease in one or more dimensions of concrete by solidification, cooling or chemical transformation. Shrinkage deformation in concrete mostly occurs at early age and can be divided into many types based on the factors affecting the volume stability of concrete. The first early age shrinkage deformation occurs when concrete is setting and starts hardening in the first 24 hours (Holt, 2001).These age-based classifications of shrinkage deformation include many types of changes attributed to autogenous and drying deformation. The age-based classification also emphasizes that concrete deformation is a function of various factors such as evaporation, consumption of water by the hydration reaction, etc. These give birth to several types of shrinkages which include endogenous shrinkage, chemical shrinkage and others that are described below.

1.7.1 Drying shrinkage.

Drying shrinkage refers to loss of water from concrete resulting in the reduction of volume. This type of shrinkage is a result of inadequacy of water within the concrete due to hydration reaction, meaning to say concrete mixes with higher w/c ratios are unlikely to experience this type of shrinkage. It is however possible if the surrounding temperature is high enough to cause excessive evaporation of bleed water when concrete consolidates upon placement. This phenomenon is termed plastic shrinkage and it has a cognate relationship with drying shrinkage.

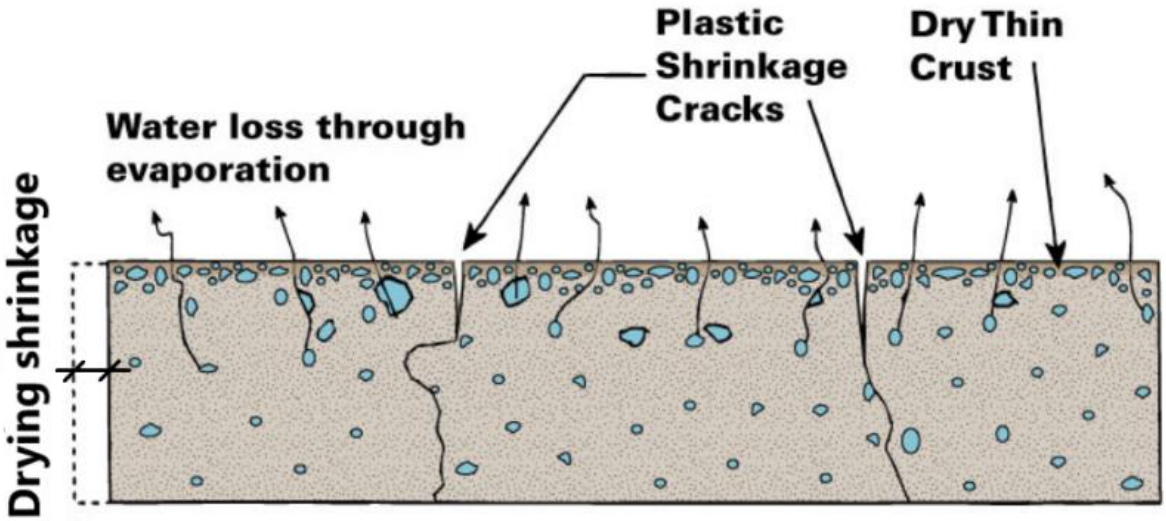

Figure 1-6 Drying shrinkage and Plastic shrinkage. (Iowa DOT, n.d.)

Water loss to the surrounding creates a capillary pressure build-up in the pore structure of fresh concrete as water from the interior of the concrete is pulled towards the surface. The internal pore structure is said to control the drying process of concrete (Ullah, 2017). The rising capillary pressure is dependent on internal pore spaces and in view of that, cement paste becomes denser with a lower w/c ratio (becomes more plastic). A build-up of pore pressure occurs as water escapes, first from the large pores. Drying shrinkage occurs if the rate of evaporation exceeds the rate of rising bleed water to surface, pores near the surface inside the concrete start losing water and drying shrinkage begins.

The water surface drops inside the concrete body in a situation where the amount of evaporating water exceeds the bleed water rising from within the concrete. At this point, the surface of the concrete can be considered as dry (plastic shrinkage), see Figure 1-6. This process develops a water pressure inside the pores and in turn causes a capillary force inside the concrete matrix (Ullah, 2017). The pressure difference between the inside and the outside of the meniscus is often called the Laplace pressure. The capillary force is described as a function of radius of curvature of the resultant meniscus between the water and air. The suction force s given by the Laplace equation is as follows, (Slowik et al., 2009) :

$$s = \frac{2\sigma}{r} \tag{1.11}$$

where: s = suction pressure (Pa)
σ = surface tension of air-water interface ($\approx 0.074\ N/m$), and
r = meniscus radius (m).

Alternatively, the *Laplace* equation may also be written as:

$$\Delta p = \frac{2\gamma}{r} \tag{1.12}$$

where: Δp = pressure difference in capillaries
γ = surface tension of water
r = radius of water meniscus.

Due to the similarity of equation (1.11) and (1.12), suction can be stated as the change of pressure of water between capillaries.

The effect of pore size (radius) has also been alluded to by Kelvin's equation (Slowik et al., 2009). Water vapour condenses at lower pressure in the capillary pores than in the atmosphere (Ullah, 2017). The relationship between the radius of pores and the relative humidity is governed by Kelvin's equation, (1.13). Pores lose moisture with relative ease as their size increase, giving a rise in capillary pressure.

$$\ln \phi = -\frac{2\sigma M}{\rho RTr} \tag{1.13}$$

where: ϕ = relative humidity,
σ = surface tension of air-water interface ($\approx 0.074\ N/m$), and
M = molar weight of water ($18\ kg/Kmol$),
ρ = density of water ($998\ kg/m^2$),
R = gas constant ($8.214\ J/Kmol$), and
r = pore radius (m).

The Kelvin equation may also be expressed as follows:

$$r = -\frac{2\gamma V}{RT\ln(\frac{p}{p_0})} \tag{1.14}$$

where: γ = surface tension of water,
V = molar volume,
R = molar gas constant ($8.214\ J/Kmol$),
T = temperature (K),
r = pore radius (m),
p = vapor pressure (Pa),
p_0 = vapour pressure of saturation (Pa)

Combining the Laplace and the Kelvin equations, (1.11), (1.13), (1.14) demonstrates the relationship between the relative humidity and suction pressure and hence the induced stresses and shrinkage. An experimental relationship has been confirmed which reveals that suction pressure increases with decrease in humidity.

$$\ln\phi = -\frac{sM}{\rho RT} \tag{1.15}$$

In case of excess bleed water on the surface of concrete, drying shrinkage may not occur, as there is a blanket cover of water allowing for evaporation at all times without increasing capillary pressure. Only when evaporation rate is higher than bleed water rising, drying shrinkage is observed. However, the questions regarding the validity of the Laplace and the Kelvin equation and the discontinuity of pore water in hardened paste require further elaboration with experimental results (Wittmann et al., 2009).

1.7.2 Thermal shrinkage.

Temperature fluctuations in concrete cause contraction and expansion which may result in thermal deformations. This type of deformation occurs both in early age and later age concrete due to either excessive heating or cooling. Hydration reactions in concrete release heat that cause concrete mass to expand. During the first 12 hours, the heat evolution rises and the concrete may expand in light of this. This stage is often followed by concrete cooling when the concrete mass adapts to the ambient temperature, which causes contraction or

shrinkage of concrete. The thermal fluctuations which result are a problematic especially if the temperature changes are too high. It is also detrimental if a large temperature gradient exists over concrete's cross-section. Part of the thermal expansion is non-elastic and appears as early-age deformation (Ullah, 2017). The temperature gradient creates differential strain and drying between layers of concrete casted at separate occasions. In mass-concretes with massive cross-sections, it takes a sufficiently longer time to achieve thermal equilibrium and therefore the problem of temperature gradients is more pronounced.

The hydration of cement is an exothermic reaction and by consequence the more cement there is in a concrete mix the greater the heat generated. Cement alone however does not govern the thermal deformations, the types of aggregates, w/c ratio, the percentage of admixtures and ambient conditions also play an important role. The overall hydration-based temperature effect is expressed in the form of a coefficient of thermal expansion (CTE) of concrete (Sellevold & Bjøntegaard, 2006). Similar to hydration reactions, CTE is a dynamic property, a function of time. It should be noted that as concrete undergoes different developmental stages, there is a continuous evolution in the physical mass of concrete before it becomes hardened and due to this, the CTE also rapidly evolves in the early stages and later it becomes more stable. Estimations of the CTE have been proposed by many researches, the (CEB-FIP, 1993) model code for concrete structures has given the following expression for calculating thermal expansion with relation to CTE:

$$\varepsilon_{ct} = \alpha_T \Delta T \tag{1.16}$$

Where: ε_{ct} = thermal strain,
ΔT = temperature change (K),
α_T = Coefficient of Thermal Expansion (CTE), (K^{-1})

A CTE value of $10\times 10^{-6}\ K^{-1}$ is used commonly for structural analysis purposes (quartzite aggregate). In the model code, it is stated that the CTE depends on aggregate types and moisture state of concrete. However, this CTE is an oversimplification of the thermal deformation phenomenon.

The CTE of water is at 23 °C is 237×10^{-6}/°C (Kell, 1975). Fresh concrete at early age is more fluid, therefore, a high value of CTE is expected. The cement paste and aggregate have different CTE. The cement paste CTE varies from 10×10^{-6} to 20×10^{-6} per °C and linear CTE for air-cured concrete with gravel and limestone is $13.1\times 10^{-6}$and 7.4×10^{-6} per °C, respectively (Neville & Brooks, 2010). See Figure 1-7
The CTE for gravel and limestone concrete is with a 1:6 cement-to-aggregate ratios. The CTE in concrete is a resultant of the CTE for cement paste and aggregates. Greater cement-to-aggregate (c/a) ratio in a mixture will result in a lower CTE. Within the cement paste, CTE can be further classified as true Kinetic coefficient and swelling pressure. The swelling pressure is the effect of decreasing capillary tension of water due to the increasing temperature. During

heating, moisture is transferred from the gel to capillary. Conversely, during cooling, the moisture diffusion occurs from the capillary to gel.

The moisture condition of the cement paste only contributes to the thermal deformations when the paste is partially saturated. If the paste is dry, capillaries are unable to supply water to the gel. Similarly, when the paste is saturated, there is no water meniscus in the capillary. In both these extremes, the effect of a temperature change is not observed.

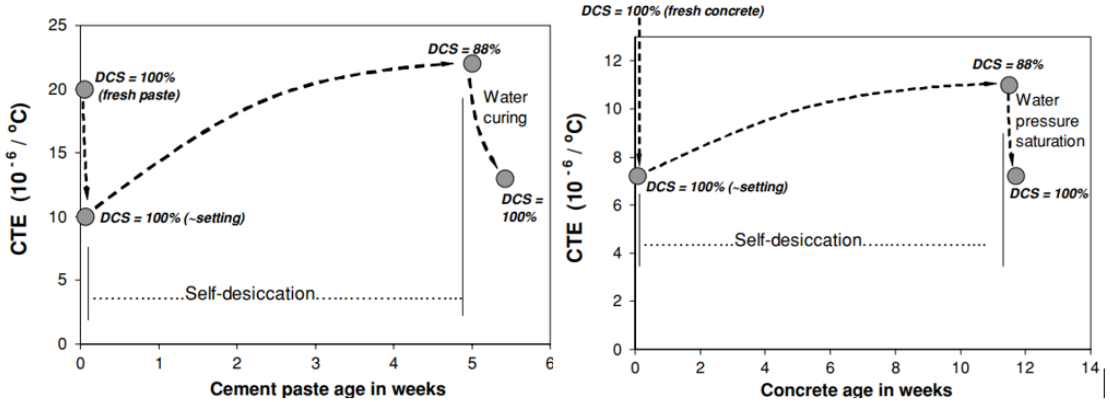

Figure 1-7 Effect of the degree of capillary saturation (DCS) on the (CTE) of cement paste and concrete. (Sellevold & Bjøntegaard, 2006)

1.7.3 Autogenous shrinkage.

Autogenous shrinkage is considered as the external-macroscopic volume reduction of hydration cement paste driven by chemical shrinkage (Klemczak & Knoppik-Wróbel, 2011). It is a type of shrinkage where loss of water is prevented. During hydration, water is consumed in the process and causes internal drying which in turn results in reduced material volume. At the early stage, when the concrete is still soft, autogenous shrinkage is only attributed to the chemical changes driven by hydration of cement particles, but at a later stage (after approximately 5 h), it is mostly due to self-desiccation, which is intensified by certain mix ingredients (silica fume and superplasticizer) and low w/c ratio. (Safiuddin et al., 2018), see Figure 1-8.

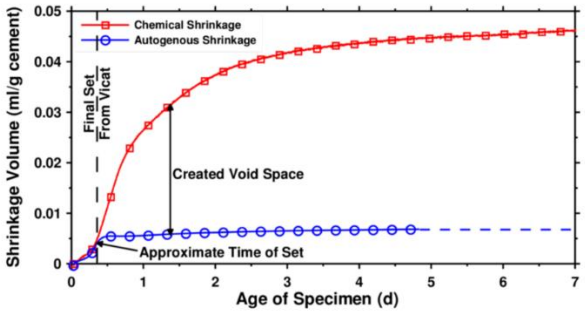

Figure 1-8 Evolution of autogenous/chemical shrinkage over time. Derived from (Jensen, 2005)

This type of shrinkage is to not be mistaken to drying shrinkage as autogenous shrinkage is not as a result of water loss to the environment. Cement hydration reactions are the greatest factor causing autogenous shrinkage. There's a significant generation of voids due to water use up in hydration as the products of hydration are said to occupy lesser space than raw materials and an overall shrinkage occurs. Therefore, autogenous shrinkage is part of the chemical reactions that occur between the raw materials of concrete. The outcome of the chemical reactions that form up the hydration products translates as macroscopic shrinkage deformation, a situation where the volume of the reacting materials is more than that of the final product (Le Chatelier theorem). This can be measured as a linear change of length. Unlike drying shrinkage, it cannot be controlled by curing or casting techniques. (Ullah, 2017)

Various names have been given to this type of shrinkage deformation. They include autogenous deformation, Le Chatelier shrinkage (although this is mostly attributed to the chemically induced autogenous shrinkage only), volume contraction, bulk shrinkage, indigenous shrinkage, self-desiccation shrinkage, and autogenous volume change (Justnes et al., 1996). As mentioned earlier, autogenous shrinkage is generally associated with concrete composites of low water-to-cement (w/c) ratio. Therefore, there is a higher risk of autogenous shrinkage in high-strength and high-performance concretes due to the relatively low w/c ratios associated with them. Before, it was ignored as w/c ratios in concrete where usually high. With the advent of high strength and ultra-high strength concrete mixtures and the use of admixtures, concrete with low w/c ratio became possible and with less free water (w/c) in the mixture, autogenous effects have become more and more apparent.

As described in (1.7.1), during the hydration process, free water is utilized and self-desiccation may occur which is defined as localized drying of internal pores of concrete. As stiffening continues, a weak skeleton is formed, which is able to resist the tensile effects of shrinkage deformation. Capillary pressure starts rising in the pores when the fresh concrete gains considerable strength, which takes over as the cause of shrinkage. The meniscus surface moves between the pores to keep this pressure mechanism until a breakthrough pressure or critical pressure reaches, see Figure 1-9. After this, the pore water is redistributed notwithstanding the continuous suction or rising**.** (Ullah, 2017)

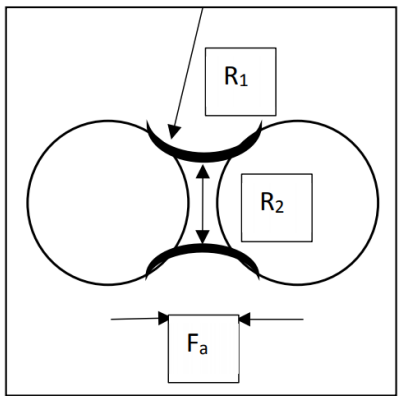

Figure 1-9 Liquid filled joint causing attraction between two spherical bodies.(Ullah, 2017)

The pressure can be calculated using Gauss-Laplace equation for the capillary pressure as presented:

$$P_c = -\gamma(\frac{1}{R_1} + \frac{1}{R_2}) \quad (1.17)$$

where: γ = surface tension of the liquid

R1 and R2 are the main radii of the curvature of the surface of the liquid. (Slowik et al., 2009)

Particles separated by a liquid film are under action of attractive forces, see Figure 1-10. For two spheres with radius R held together by a liquid ring of diameter R, the attractive force f_a is as follows.

$$f_a = \sigma\pi R \quad (1.18)$$

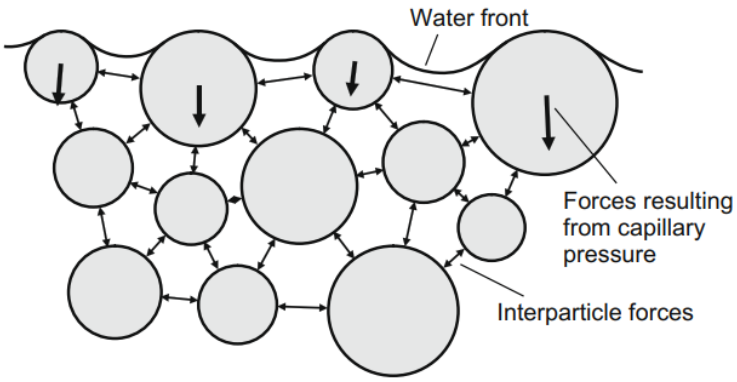

Figure 1-10 Forces acting on solid particles: interparticle and capillary forces. (Slowik et al., 2009)

Concrete with adequate w/c ratio or subjected to proper curing does not experience capillary pressure development or increase due to presence of bleeding water on the surface of fresh concrete. This means that the driving factors for the autogenous shrinkage keeps evolving with the hydration reactions as the concrete gains strength.

1.7.4 Chemical shrinkage or Le Chatelier shrinkage.

As mentioned earlier on, initially autogenous effects are purely chemical, since in Liquid stage chemical shrinkage reduces the volume of the mix and voids are created. In the hydration reaction of cement, the cement matric contracts and the volume of hydrated cement becomes smaller than that of anhydrous cement.(Zreiki, 2009)

$$\Delta V = (V_{Ci} + V_{Wi}) - V_{hy} \quad (1.19)$$

This volume reduction is usually between 8 to 10% of the total initial volume of water and cement (Briffaut, 2010). Chemical shrinkage is based on the initial and final volumes of

hydration reactants and products. The general expression for percentage chemical shrinkage is given below:

$$C_s = \frac{\Delta V}{V_{Ci} + V_{Wi}} \times 100\% \quad (1.20)$$

Where: C_s = percentage chemical shrinkage

- V_{Ci} = volume of cement before mixing
- V_{Wi} =volume of water before mixing
- V_{hy} = volume of hydrated products
- ΔV = volume difference between reactants and products

1.8 Creep in early age concrete.

Creep is a time - stress dependent deformation which occurs on prolonged application of a load. In some context it might not be qualified as an early age behavior of concrete, but the problems of creep all start following the concrete gaining sufficient strength to carry load. This load ranges from self-weight or service and imposed dead loads in the case of specialized structures designed to carry loads at very early age.

Figure 1-11 Cracked concrete structure due to creep. (Online Civil Engineering, n.d.)

Concrete properties such as creep and its associated relaxation play a very important role in the reduction of build-up of self-induced stresses and in assessing the risk of cracking, of interest are the early days after placement. During the hardening of concrete, relatively small compressive stresses and then significant tensile stresses are generated in the restrained concrete, accompanied by both the compressive relaxation and then tensile relaxation.

Depending on the ambient humidity, one can distinguish between two types of creep, namely basic creep and drying creep. Basic creep is creep occurring under no moisture exchange between the concrete and the environment. During drying and with moisture

exchange between the environment and the concrete, there is an additional creep component referred to as drying creep or Pickett effect. Drying creep is usually much greater than basic creep under moisture conditions. This drying creep is influenced by the tensile stress induced in the outer part of a concrete specimen with resultant cracking.

1.8.1 Instantaneous deformation

As is the case with a plethora of any other construction materials, concrete exhibits, to a certain degree, an elastic behavior when a load is first applied. The strain at loading is mainly elastic strain with a small inelastic component, and corresponds to the static modulus of elasticity at the age at which the load is applied. However, it should be noted that in a stress-strain experiment a certain time is used to carry out the loading processes. The loading time will increase the strain due to the creep of concrete. Consequentially the response will also include a certain creep deformation depending on the rate of application of load. This deformation is usually named the instantaneous deformation. The time duration for application of load in determination of the elastic modulus is not defined in all the practical codes, making it difficult to compare test data published in literature. As such what we call instantaneous depends on our definition or rather the available equipment and the chosen procedure. The instantaneous deformation defines the modulus of elasticity of the concrete.

1.8.2 Creep recovery

When the sustained stress is removed, the strain decreases immediately by an amount defined to be the elastic deformation at the time concerned, see Figure 1-12. This immediate reduction is called initial recovery or instantaneous/immediate recovery. Since the young modulus at the given time is higher than its value at the loading age, and due to possible non-elastic deformations (irreversible) at loading, the instantaneous recovery is less than the elastic deformation was on loading. The instantaneous recovery is followed by gradual decrease in strain, called creep recovery, see Figure 1-12. Initial recovery corresponds to instantaneous elastic deformation at the unloading time, and creep recovery corresponds to delayed elastic deformation. The development of recoverable creep exhibits an initial rapid increase with time but reaches a constant value in contrast to creep which continues indefinitely.

Creep is partly reversible. The irreversible deformation (residual deformation) is relatively large in most cases. Creep recovery is smaller, but important in prediction of deformation in the concrete under variable stress.

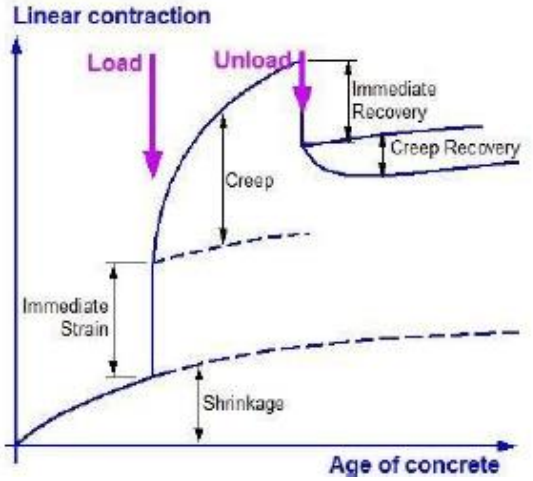

Figure 1-12 Elastic and creep deformation of mass concrete under constant load followed by load removal. (Gambali & Shanagam, 2014)

1.8.3 Mechanism of creep

There is a general agreement amongst scholars that creep of concrete has its roots embedded in hydrated cement paste and, at high stress, also in failure of the paste-aggregate bound. Creep is believed to be related to internal movement of adsorbed water, a phenomenon which has internal seepage at play. It is also common knowledge that basic creep decreases strongly with decrease in moisture content.

Many theories of the creep mechanism have been proposed in the past decades, and presented (Neville et al., 1983). These include; mechanical deformation theory, plastic theory, viscous and visco-elastic theory, elastic after-effect theory, solid solution theory, seepage theory and micro-cracking theory. In the field of research on creep there is a consensus that none of the proposed theories is capable to account for all the observed phenomena. None of them can explain to satisfactory terms the behavior of concrete under various environmental conditions and under various states of stress. A couple of mechanisms are involved in the actual creep. According to American Concrete Institute, referred in (Neville et al., 1983), the main mechanisms, which describes creep, are:

- Viscous-flow of the cement paste caused by sliding or shear of the gel particles.
- Consolidation due to seepage and redistribution of pore water under stress.
- Delayed elasticity due to the cement paste acting as a restraint on the elastic deformation of the skeleton formed by the aggregate and gel crystals.

1.8.4 Factors affecting creep

1.8.4.1 Concrete age

Concrete age at the time of application of the load is a major extensive factor, which influence the visco-elastic behavior of concrete. This effect at early ages is of high interest in

connection with thermal stress analysis and pre-stressing. The general pattern of influence of the age at application of load on creep. The rate of creep during the first weeks under load is much greater for concrete loaded at an early age than for old concrete and after about 28 days under load, the age at application of the load is a non-factor.

1.8.4.2 Stress magnitude

There is enough evidence that creep is proportional to the applied stress until a certain stress threshold and is inversely proportional to the stiffness of concrete at the time of application of the load, alternatively said, the magnitude of creep is related to the instantaneous deformation. The stress level is generally expressed by stress as a fraction of strength, and the ratio stress/strength is considered as a practical approach to express the relation between creep and stress level for different concrete qualities.

1.8.4.3 Elevated temperatures

A wide range of findings on elevated temperatures has shown that the creep deformation increases significantly with increasing temperature. The influence of temperature on time-dependent deformations has been a subject of interest in the building of pre-stressed concrete pressure vessels in nuclear reactors since the service conditions involve quite high temperatures. This is due to the fact that the pre-stressed concrete structures undergo more creep in hot weather than in cool air.

The influence of temperature is even larger at early age (since any increase of temperature means faster hydration) and thus it is of interest in thermal stress analysis. Creep increases with increasing temperature, but the effect is offset by the fact that a temperature increase also accelerates hydration, which in turn reduces creep. Consequently, a higher temperature tends to increase the creep rate, but will also indirectly reduce the creep. Dependent on the concrete age, the former effect is usually higher than the latter one.

In literature, it is reported that the strength and modulus of elasticity are affected by elevated temperature during the period of creep testing, and this will certainly affect the creep. At normal constant temperature the modulus of elasticity of sealed concrete increases slightly with age, while the E-modulus of drying concrete can decrease due to the loss of loadbearing water.

The most important factors concerning influence of elevated temperature on creep development by time are:

- Temperature prior to loading
- Temperature during loading
- Temperature variation during loading

Clarity is important in distinguishing between the temperature during the period of curing preceding the application of load and the temperature while the concrete is under load. Increase of temperature prior to loading for a long time will definitely accelerate the hydration process in concrete, and as a consequence the concrete gains a higher degree of maturity as given by (Neville et al., 1983).

We have to distinguish between the temperature during the period of curing preceding the application of load and the temperature while the concrete is under load. Increase of temperature prior to loading for a long time will accelerate hydration process in concrete, and as a consequence the concrete gain a higher degree of maturity.

In a case of creep deformations under varying temperatures no thermal equilibrium is obtained. A change in temperature during the period of sustained loading, has the creep rate increasing and influencing the rate of aging of the concrete. Furthermore, is the fact that temperature change leads to redistribution of inherent moisture in the cement paste as well as structural change which are equally vital for creep. (Illston & Sanders, 1973) describe the rapid increase in creep, due to a positive change of temperature, as transitional thermal creep which is approximately independent of maturity, and is zero when the temperature decreases or when the temperature is raised to the given level for a second time. To sum it up, a drop in temperature does not give any creep recovery. Literature is also awash with findings that entail that increasing the temperature by several steps gives a higher creep than a steady temperature after a certain period of loading.

1.8.4.4 Influence of water/cement ratio

Any change in w/c ratio will affect the Young modulus and the strength of the concrete. Keeping the initial applied stress constant, a mix with a low w/c ratio has a greater Young modulus and strength than a mix with a high w/c ratio.

1.8.4.5 Ambient relative humidity

In general creep is higher with lower relative humidity. Shrinkage occurring in specimens during the early stages after the application of the sustained load is the main culprit for this. Thus, the enhanced creep of concrete due to drying is due to the additional drying creep or called Pickett effect. Under dry conditions, creep develops at a higher rate in the initial period after loading than under more humid conditions. Reduced relative humidity leads to reduced creep for specimens in moisture equilibrium with the environment before loading (basic creep).

1.8.4.6 Aggregate

It is ascribed that, it is the hydrated cement paste which undergoes creep, and thus the primary role of aggregates in concrete is restraining of creep and shrinkage. As such, creep is therefore a function of the volumetric content of cement paste in concrete and thus volumetric content of aggregates. The end result is an inverse proportionality between aggregate contents and creep.

Certain physical properties of aggregate influence the creep of concrete as well. The modulus of elasticity of concrete is probably the most important factor. The higher the modulus the greater the restraint offered by the aggregate to the creep of the hydrated cement paste. According to (Neville et al., 1983) the higher creep of concretes made with lightweight aggregates reflects only the lower modulus of elasticity of the aggregate, but of course water in the lightweight will play a role also.

1.9 Conclusion.

Mass concrete is prone to thermal cracking and reduced durability, largely because of two combined factors namely, considerable hydration heat and relatively lower conductivity concrete material to create adiabatic conditions in a mass concrete structure. These give rise to shrinkage and creep. Of course, there are other extraneous factors such as poor workmanship that might be responsible for cracking but they were not of importance in this piece of work. There is a direct relationship between structure size and its vulnerability to cracking. In light of this, bulk concrete has two important thermal characteristics which are, an excessive temperature rises and the temperature differential. Due to the thermal movement restraint of structural elements for mass concrete, the temperature differential between adjacent positions should not be significant between the centre of the concrete section and the surface. Otherwise, it may be constrained to increase the interior, exterior, or both restraints and enhance the probability of cracking.

Chapter 2: Temperature control in mass concrete.

2.1 Introduction.

The early age behaviour of concrete can be controlled to some extent. By employing several measures and methods, the construction industry has learnt to mitigate these effects. From precooling methods, post cooling methods and even limiting the percentage of cement in concrete mixes, all these methods have helped reduce the undesirable early age effects in concrete. In this section we are going to have an in-depth discussion articulating on ways of addressing the early age hydration problem.

2.2 The need for temperature control in mass concrete at early age.

If cement and pozzolans did not generate heat as the concrete hardens, there would be little need for temperature control. In a lion's share of cases, this heat generation and subsequent temperature rise occurs at telling speeds that propagate the hardening of concrete in an expanded condition. And in simultaneous fashion, an increase in the elastic modulus is accompanied by a gradual temperature rise for several days after casting. We could disregard such detrimental circumstances if the entirety of the placement mass could be:

- Maintained at a constant temperature from the core to the outer and exposed surfaces
- limited to a temperature ceiling that is well-nigh of its cooled stable temperature
- supported without restraint (or supported on foundations expanding and contracting in the same manner as the concrete)

It is an engineering vantage position that none of the above-mentioned conditions can be achieved in isolation or as a couple. We can, however, to a certain extent achieve the first and second conditions in most constructions but constructing structures or elements of a structure with limited restraints is very difficult to achieve. Maintaining constant concrete temperatures throughout the structure has been accomplished on a limited scale for extremely critical structures. The implored techniques have been phase casting and minimizing temperature differences between two concrete mixes placed at different times.

2.3 Structural conditions.

The size, type, function of the structure, the climatological environment, and the degree of internal and external restraints imposed on a structure all dictate the extent of vulnerability of the structure with regards to early age behaviour of concrete. Below are the two primary concerns to look at when trying to counter resultant deformations in concrete at early age.

2.3.1 Restraints

Restraint conditions are the primary cause of cracks due to hydration heat evolution in concrete particularly in massive structures. They are also the hardest to eliminate or deal with as mentioned above. It is important to note that without the various types of restraints imposed on the concrete masses, hydration heat would not be a nightmare to engineers as is the case.

2.3.1.1 Internal restraint

Internal restraints occur when there is a temperature difference between the core and the surface of the concrete during the expansion and contraction phase, as shown in Figure 2-1. The temperature at the surface is often cooler than in the core, preventing the inner parts to expand. This results in internal restraint of the structure and the risk of surface cracks arises. Depending on when the cracks occur, they may be permanent. If they occur in the expansion phase, they usually close due to the self-healing properties of concrete. If they occur in the contraction phase, they may be permanent. (Lagundžija & Thiam, 2017)

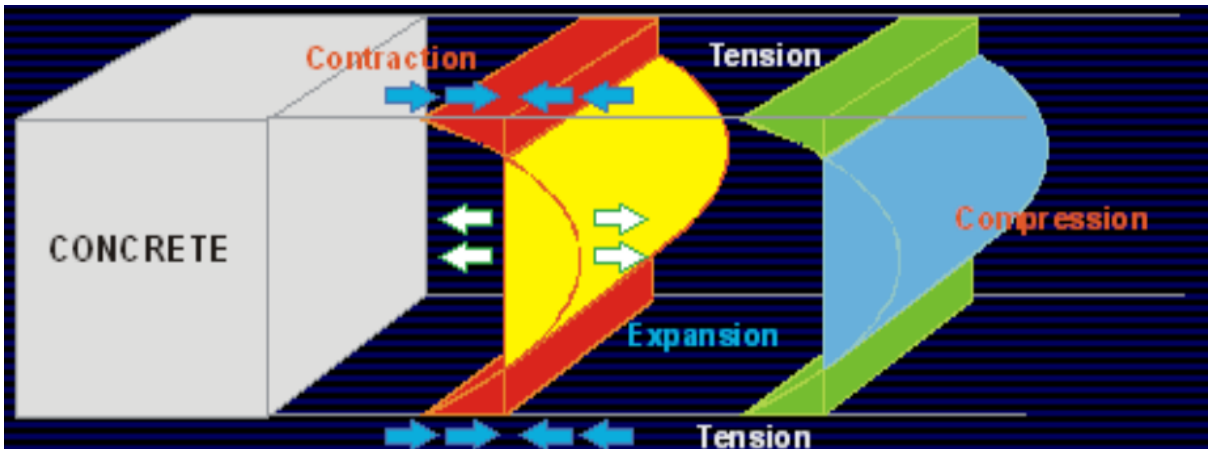

Figure 2-1 Effect of heat generation from cement hydration on mass concrete placement. (Lagundžija & Thiam, 2017)

2.3.1.1.1 The expansion phase

The expansion phase occurs at the beginning of casting and acts until the structure reaches its maximum temperature. During this time the concrete is more plastic with a low elasticity modulus and is expanding due to temperature rise within the structure. As the temperature

is rising, the stiffness of the concrete increases, contributing to compressive stresses at the core of the concrete and tensile stresses close to the surface.(Lagundžija & Thiam, 2017)

2.3.1.1.2 The contraction phase

The contraction phase follows the expansion phase and it is when the temperature is starting to decrease. However, not all the cement would have reacted yet with water and there will still be heat generation within the concrete although it will not be enough to sustain expansion. The compressive stresses at the core of the concrete change into tensile stresses owing to the significant temperature reduction. This cyclic behaviour exchange of contraction and expansion between the concrete core and surface is a classic example of internal restraints within concrete.

2.3.1.2 External restraint

When a structure is cast against an adjacent structure such as previously cast concrete members or a rock, the adjacent structures cause restraints in the new cast concrete component and prevent it from freely contracting and expanding, as shown in Figure 2-2. The restraint is largest at the joint between the structures and is decreasing with increasing distance from the joint. With external restraint, the risk of cracks is amplified as the structure is not free to move. The cracks will appear orthogonal to the restraint edge.(Lagundžija & Thiam, 2017)

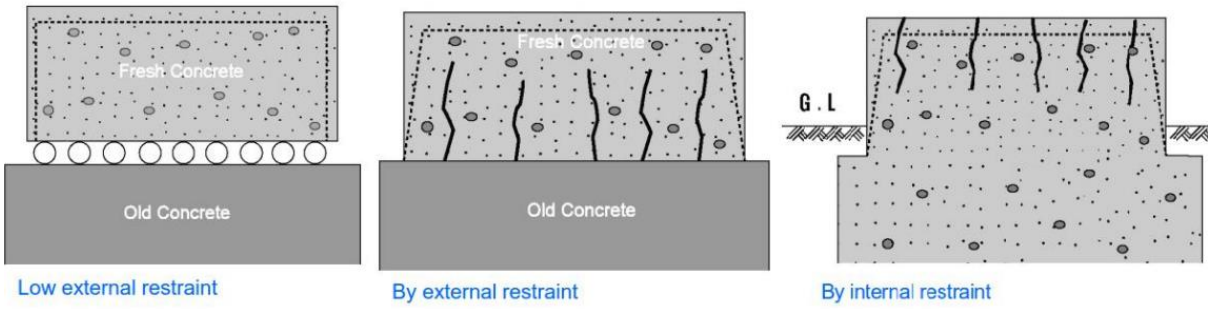

Figure 2-2 Restraint on mass concrete. (Kaium, n.d.)

2.4 Cooling of concrete.

The need to control erratic volume changes induced primarily by temperature variations in vast and bulk concretes has culminated the development of various cooling and insulating systems for use in mass concrete construction. There exist two broad temperature control methods in concrete, namely:

- Precooling methods
- Post cooling methods

2.4.1 Precooling methods

One of the leading influences on quashing of thermal cracking is the control of concrete placing temperatures. It is deemed that, the lower the temperature of the concrete when it passes from a plastic phase to an elastic phase undergoing hardening, the less the tendency for it to crack. According to (ACI, 1998), in massive structures, a 6℃ lowering of the placing temperature below the average air temperature will result in a 3℃ decrease of the maximum temperature reached by the concrete.

Table 2-1 Example of a $1\ m^3$ mass concrete mixture and its water equivalent. (ACI, 1998)

Ingredient	Batch weight (kg)	Specific heat capacity $(kJ/kg.K)$	Batch heat content(kJ/K)	Water equivalent (kg)
Coarse aggregate	1672	0.75	1254	300
1% moisture	17	4.18	71	17
Fine aggregate	528	0.75	396	95
5% moisture	26	4.18	109	26
Cement	117	0.88	103	25
Admixtures (Fly ash)	50	0.84	42	10
Batch water	82	4.18	343	82
Total	2492		2318	555

2.4.1.1 Batch water.

Measures to reduce maximum hydration temperature may be implemented in batch water itself. By assuring the temperature of batch water is considerably low, the maximum hydration temperature reached by the concrete can be significantly reduced. There are two ways in which we can achieve this:

2.4.1.2 Using ice as batch water

The use of ice is one of the most efficient and basic methods to lower concrete placing temperatures due to its high energy absorption properties as it changes from solid to liquid. $1kg$ of ice absorbs $334\ kJ$ when it changes from ice to liquid water. This method uses block

ice that is crushed or chipped and added directly into the mix. It is of paramount importance to ensure that all the ice melts prior to the conclusion of mixing. Also, sufficient mixing time should be allowed to adequately blend all the melted ice into the mix and attain homogeneity. Homogeneity in the concrete mix and buffers void development. Where aggregates are processed dry, there is need to introduce a percentage of batch water in liquid state which can be achieved by spraying chilled water on the coarse aggregates while on the conveyor belt en-route to the batch bins (ACI, 1998). There is sufficiently enough moisture on the aggregates when aggregates are processed wet, therefore in this case all the batch water can be added as ice. Taking the concrete mix in Table 2-1, using the entire $82\ kg$ of batch water as ice, the melting of the ice water would lower the temperature of the concrete mass by about $12℃$ as illustrated below:

$$\Rightarrow \frac{82(kg)\times 334(kJ/kg)}{555kg(water\ equivelant)\times 4.18(kJ/kg.K)} = 11.8K = 11.8°C \quad (2.1)$$

2.4.1.3 Chilled batch water

We can directly chill the batch water to a desired temperature which in turn significantly reduces the maximum hydration temperature of concrete. According to (ACI, 1998), $1Kg$ of water absorbs $4.18\ KJ$ when its temperature is raised by $1℃$. Considering the high specific heat capacity of water relative to other materials, a unit change in temperature of the batch water has approximately five times an effect on the temperature of the concrete as that of the cement or aggregates. This approach is also relatively economic as equipment for chilling water is less complicated and cheaper than ice-making equipment. Practically, batch water is produced consistently at $2℃$ or slightly lower. Using the mass concrete mixture in Table 2-1, chilling $82\ kg$ of batch water from $21℃$ (average adiabatic temperature) to $2℃$ will reduce the concrete temperature by about $3℃$. This is calculated using the following expression:

$$\Rightarrow \frac{82(kg)\times(21-2)°C}{555kg(water\ equivelant)} = 2.8°C \quad (2.2)$$

2.4.1.4 Aggregate cooling.

Aggregate cooling is one of the most effective precooling methods since aggregates makeup the greatest portion of concrete mixtures. The method has seen its application in projects such as the Chirkey Hydroelectric plant in Russia. (Shitov et al., 1976)

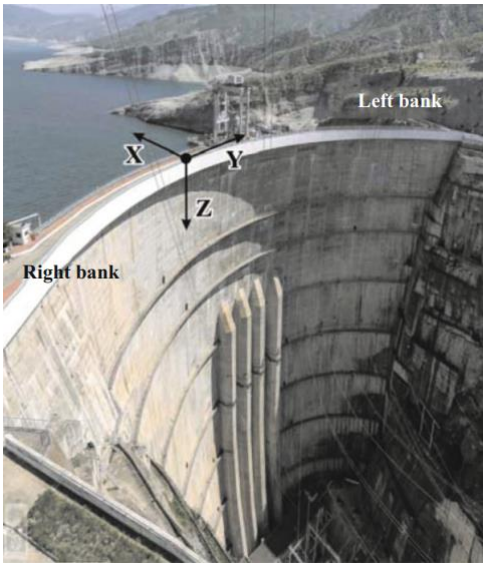

Figure 2-3 The Chirkey Dam, Russia. (Liseikin et al., 2019)

The only drawback of using this approach is that most rock minerals have a relatively low unit heat capacity and thus sometimes impairs the efficiency of the method in question. With regards to mass proportions, aggregate temperature has the most important influence on concrete temperature. Adiabatic temperatures obtained in mass concrete construction render temperature control of aggregates imperative. Several ways of aggregate cooling have been established over the years, namely:

2.4.1.5 Cold weather aggregate processing.

Everything considered and in the grand scheme of mass concrete projects, aggregate processing occurs in phase with concrete production and placement. Structures constructed from rolled compacted concrete (RCC) require considerable portions of the concrete aggregates to be processed and stockpiled before placement operations resume. This is done to maintain a smooth flow of operations given RCC placement occurs at a faster rate than that of aggregate production. In a bid to control costs and meeting demand, significant temperature reductions can be realized by processing aggregates during the colder winter seasons, at locations where a marked winter season occurs.

2.4.1.6 Fine aggregate processing in chilled water.

Using chilled water to cool fine aggregate is probably the most efficient way of reducing fine aggregate temperature. Fine aggregates cooled by this method gains heat quite slowly following wet classification because of the moisture they carry and the possibility for evaporation.

2.4.1.7 Vacuum cooling of aggregates

Vacuum cooling of aggregates thrives on the low boiling point of water at lower atmospheric pressure, and the great heat absorptive capacity of water when it changes from liquid to vapour. This cooling method is applicable to aggregates of different sizes ranging from fine aggregates to coarse aggregates. Aggregates are best treated moist or when they contain

sufficient water to absorb all the heat that must be freed from the aggregates. The moist aggregates are fed into a pressure vessel that can be sealed at both the top inlet and the bottom outlet. A vacuum is created in the chamber by steam fed diffusion pumps. Also, adsorption water on the aggregates aids evaporative cooling.

2.4.1.8 Sprinkling of coarse aggregate stockpiles

Similar to vacuum cooling of aggregates, misting or sprinkling water onto coarse aggregate stockpiles is a cheap but limited means of reducing coarse aggregate temperature. The amount of cooling that can be achieved is directly dependent upon the cooling effect of natural evaporation. This in turn is dependent on the ambient conditions of temperature, wind, and relative humidity. This method requires adequate drainage beneath the stockpiles for good evacuation of accumulating water, although in theory, water sufficient to balance evaporation rates is necessary.

2.4.1.9 Liquid nitrogen

An alternate method for cooling batch water and creating an ice/water mixture employs liquid nitrogen, an inert cryogenic fluid with a temperature of $-196℃$. The liquid nitrogen is directly poured into the batch water storage tank from a cryogenic storage tank to bring the water temperature down to $1℃$, see Figure 2-4. To promote greater cooling of the concrete, liquid nitrogen is injected into the water. This is done prior to the water entering the concrete mixer, where the liquid nitrogen will cause a portion of the water to freeze. The amount of ice produced can be varied to meet different temperature requirements. The use of nitrogen cooling systems has proven to be very successful particularly in cases where there are automated control mixing operations. Liquid nitrogen can also be injected directly into mixer drums, although this approach may require that the mix time be prolonged.(ACI, 1998)

Figure 2-4 Injection of nitrogen directly into a concrete mixer.

2.4.1.10 Taking advantage of Placement area conditions.

Under extreme hot weather, precooled concrete can absorb ambient heat and solar radiation during placement. This in turn escalates an already existing problem associated with

hydration resulting in an increase of the effective placing temperature and the consequent peak temperature. Such an increase in temperature can be minimized or eliminated by taking charge of the temperature of the placing area via fog spraying and/or shading. Placing at night is another masterstroke which reduces the effects of hot weather and radiant heat.

2.4.2 Post cooling

This system is based on reducing the maximum temperature difference between the core of mass concrete and its surface after placing. To arrive at our goal of minimizing potential cracking we either aim at slowing down the rate of heat dissipation from the surface of the concrete or lower the internal temperature of the concrete.

2.4.2.1 Pipe cooling

World over, cooling pipes are often used to cool concrete and confront the global problem of concrete cracking at early age. The principle is to lay thin pipes in the structure. As concrete casting kick-starts, cold water is pumped into these pipes to limit the temperature rise inside the concrete during the hydration. The advent of this method was at the construction of the Hoover Dam in the 1930's (Qian & Gao, 2012), and with time it has seen many other dam concretion projects profiting from this technique. The Plattsmouth Bridge built over the Missouri river (Figure 2-5), consisting of 19 massive concrete elements is a classic example. Cooling pipes were used to cool four of those massive elements. (Lagundžija & Thiam, 2017)

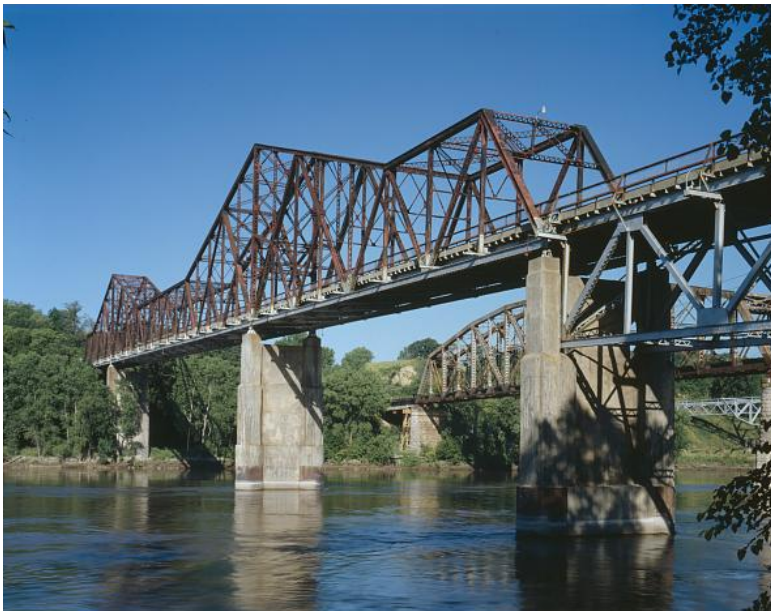

Figure 2-5 Plattsmouth Bridge (US-34 Bridge) over the Missouri river. (Library of Congress)

Scholarly work by (Qian & Gao, 2012) show that the main criteria affecting the efficiency of a pipe cooling system are:

- The water flow and its direction inside the pipes.
- The initial temperature of the water.
- The spacing and layout of the pipes.

- The physical characteristics of the pipes such as the diameter, the length and type of material.
- The cooling sequences.

The water flow is set in a way that ensures a good water exchange in the pipes. During the cooling process, the water gets warmed up by absorbing the heat from the hydration of concrete. If the flow is not high enough, the water quickly approaches the concrete temperature. Consequently, heat transfers between the water and the concrete come to a halt. Reaching such an unfavourable fate renders system inefficiency (Charpin et al., 2004).

The choice of the pipe material is equally important. Pipes that have a low heat of resistance are ideal for efficient heat exchange. The resistance depends on thermal characteristics and on the pipe dimensions. Thus, the material should have high heat conductivity to ease the heat transfer from the concrete to the water through the pipe wall. Dimension-wise, many small pipes are preferred to few large pipes. Experimental results obtained by using an important quantity of small diameter pipes were richer than the results obtained with few larger diameter pipes. As the number of pipes increase the surface area exposed and in contact with the heating concrete increases and the cooling capacity inevitably augments, thanks to more heat absorption (Charpin et al., 2004).

Cooling pipes are not easy to handle and include a lot of risks especially in regions with very cold winters. The pipe entrance can freeze due to low ambient temperature. To counter the freezing, the pipes are warmed at the entrance so that water circulation is not blocked by ice which forms. The aforementioned is a positive step in having an efficient cooling system. At all times the pipes have to be functional and a high level of carefulness is needed. It's no fluke that several engineers within the domain have given a rebuttal on how this method is way too expensive for the results it gives as many factors have to be taken into account to have good cooling results.

It is regrettable that this method of cooling can cause severe cracks in the concrete around the cooling pipes due to a high difference in temperature between the circulating water and the concrete. The eventual temperature gradient creates significant tensile stresses which may lead to cracks. To nib such a fatality, a reduction in the water flow results in the stress and thus the crack formation around the pipes are lowered. Cooling the structure slowly ensures a balance between having an efficient cooling system and as low stresses as possible near the pipes. (Qian & Gao, 2012)

Water is the primary cooling fluid of choice. Other scientific findings point to contemporary fluids such as air to be useful. However, cooling with air should be on a pretext that the diameter of the pipes increase to give the desired effect (Hedlund & Groth, 1998). A larger specific heat capacity of water than air is the reason behind this. Putting it into perspective,

at $25\ °C$, the specific heat capacity of water and air are 4.18 and $1.005\ kJ/kg.K$ respectively. If we are to have efficient cooling, more air should then circulate in the pipes. In all instances, everything comes down to what is cheaper in context, for instance in hydropower plant constructions, using water is much cheaper given the access to cold water is easier and readily available.

2.4.2.2 Insulation

The insulating surface method is believed to be the most effective and efficient solution to avoid the thermal cracking hurdle at early age. Insulation mats are attached to the mass concrete's surface to crucially reduce the maximum temperature difference between the core and perimeter by retaining heat at a concrete surface. Since the tensile stresses on the surface of mass concrete curtail as the maximum temperature differential decreases, the possibility of thermal cracking subsequently decreases.

Insulation blankets or cooling pipes are often installed even in the case of low heat concrete mixes to control temperature based on the weather conditions. This is so because an assortment of techniques is always faithful in controlling cracking. For the majority of mass pours, surface insulation does not appreciably increase the maximum concrete temperature, but it significantly decreases the rate of cooling. Banking on its simplicity, insulation is inexpensive. However, delays resulting from the reduced cooling rate can be costly to the whole chain of production as insulation often has to remain in place for several weeks or longer. Removing it too soon potentially causes thermal shock and crack will be unavoidable. Acceptable temperature gradients can be maintained during different seasons of the year by varying the type of material used as the insulation mat.

A maximum tolerable temperature differential of 20 °C is often recommended for mass concrete. This temperature difference is a general guideline based on experience with unreinforced mass concrete installed in Europe more than 75 years ago. Predictably, the tolerable temperature differential is a function of the mechanical properties of the concrete, such as thermal expansion, tensile strength, and elastic modulus amongst others. Some sources have suggested that, for concrete with gravel, granite, and limestone coarse aggregates, the temperature difference limit should be 20°C, 25 °C and 31°C, respectively. The coarse aggregate should also be from a single source to limit temperature differentials in order to avoid cracking. This concept was employed in the construction of the Libby dam in Montana, USA. (ACI, 1998)

Figure 2-6 Libby Dam, Libby Montana, USA (Taylor, 2020)

2.4.2.3 Curing and other post cooling methods

Other methods such as cooling with a fine water spray (Figure 2-7), cool curing water, and shading can also be implemented. The results are however variable and do not greatly affect the interior of massive placements when the ratio of exposed surface area to volume is very small.

Figure 2-7 Fine water spray curing.

2.5 Conclusion.

Degradation of concrete due to thermal stresses and cracking is a major problem of mass concreting in the early ages due to evolution of hydration heat. In order to control the temperature and prevent excessive thermal stresses, precooling and post cooling methods can be implored, though a nexus of the two gives the best results. Because of forced cooling in pipe cooling, the temperature of the concrete near the cooling pipe is lower, however, it increases rather rapidly away from the pipe, which gives rise to a temperature gradient. This can initiate cracking in the concrete around the cooling pipe. It prompts for extreme care to be taken when using pipe cooling to obtain the best results. Potentially, this surges operational costs.

Surface insulation is arguably the best single technique which can exterminate cracking, unfortunately it slows down the construction process as a sudden removal of framework can cause thermal shocks. The aggregate precooling measures can effectively control the temperature rise in early-age concrete. Aggregate cooling is cheaper, faster and easy to implement than post cooling methods. In many instances, however, post cooling is preferred over precooling due to its accurate perdition of thermal behaviour. Depending on the context, certain methods could achieve better results in alleviating thermal behaviour in mass concrete than others. For example, phase casting is inapplicable where structural elements are primarily subjected to shear stress in a horizontal direction due to the weak bonding strength at the interlayer.

Chapter 3: Numerical Analysis of Early Age Behavior of Concrete.

3.1 Introduction.

In this section, a qualitative study on the early age behaviour of concrete will be simulated by means of mesoscopic modelling of concrete specimen using the software Cast3m. The choice to use a mesoscopic modelling method is mainly motivated by the degree of accuracy of the results as it represents characteristics closer to the actual physical ones.

3.1.1 Scales of modelling.

Numerical modeling is an essential tool in the field of analysis and the study of structures/civil engineering works. It contributes to the understanding of mechanical behavior of materials used in constructions in order to control the mechanisms causing their degradation and thus allow the prediction of their behavior under various demands. Several approaches can be adopted in order to model the behavior of an element/structure subjected to mechanical loadings. One can quote three approaches; global approach, semi-global approach and local approach, see Figure 3-1.

3.1.1.1 Global Approach.

A global approach is one that identifies an entire structure as an entity, without breaking it down into elements and/or sub elements. The principle of the approach in our instance is to consider concrete as a whole without breaking it down into its constituents or considering the behavior of individual constituents. It outputs generalized stresses and strains. It is a more suitable approach when studying a global behavior of a system without taking too much particular interest on microscopic behaviors. The main advantage of a global approach is:

- it consumes less memory on simulations and takes less time.

The main disadvantage of a global approach is:

- It does not allow for representation of finely mechanical phenomena and local responses.

3.1.1.2 Local Approach.

The local approach corresponds to the study of a detailed part of the structure. For a building, these are the parts whose dimensions are small compared to the elements.

The mesoscopic approach defines concrete as a heterogeneous material, taking each constituent of concrete as an individual entity. A representation of the material on a mesoscopic scale makes it possible to account for all the complexity of concrete behavior. The nature of the heterogeneity of concrete depends essentially on the scale of observation. If we look at the scale of the grain of sand in concrete, we can consider it as a two-phase material, with aggregates of complex shapes, of different sizes distributed randomly in the concrete

matrix. This is what interests us the most with respect to the mesoscopic modeling scale, the ability to break down the global concrete material into different constituents which can be further analyzed to give a more accurate and detailed response.

On a macroscale, concrete is traditionally considered as a homogenous material treated as such in classical finite element models. The macroscale approach does not make any assumptions about the shape of the distributions of the displacement field. The constitutive laws of materials are entirely described by local variables (stresses and strains) and are generally independent of the geometry of the structure. Modeling by the Finite Element Method (FEM) allows to access the strains at any point of the structure from the nodal displacements and the corresponding constraints are integrated into the volume of the element to access the internal forces. Plainly, the treatment of concrete as a homogenous solid is only valid when the macroscopic scale of observation is of interest and the stress strain variation in critical regions is not drastic. (Lu, 2013)

The main drawback of this approach is the large volume of calculations generated by the large number of degrees of freedom used although this disadvantage could be put to bed thanks to the progress of computer tools. The local approach is very useful for validation of the experimental behavior of a structural element or for the validation of global models.

3.1.1.3 Semi Global Approach.

This approach makes it possible to use local models of concrete and steel behavior in the framework of a simplified kinematics associated with finite elements of a beam, plate or shell type (Ile, 2000). Models of this type make it possible on the one hand, to exploit the characteristics of structural elements by reducing the size of the system of equations, and on the other to promote a faster integration of constitutive laws. The important advantage of this approach lies in the implicit coupling of bending and normal forces. This approach is best suited for the modeling of beam and column systems. For the 2D modeling of reinforced concrete walls whose behavior is controlled mainly by bending, a Euler beam element is adopted. For the 3D problems, a multifiber Timoshenko beam element having functions of higher order interpolation is adopted.

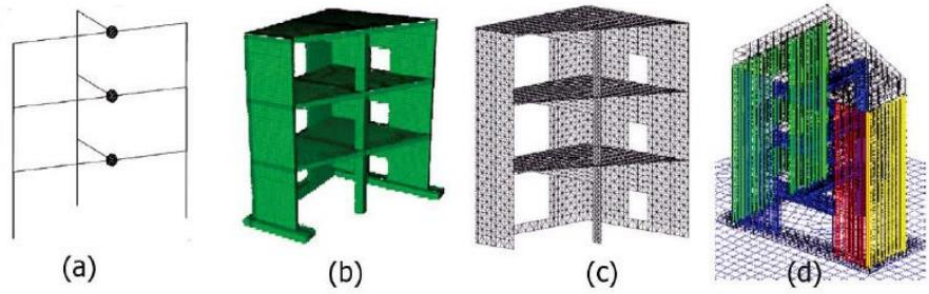

Figure 3-1 Model approaches, a) Global approach, b)-c) Local approach, d) Semi Global approach. (Lermitte, 2010)

3.2 Modelling.

Evaluating the behavior of concrete at a mesoscopic level requires the generation of a digital concrete with at least two phases, cement paste structure (matrix) and aggregates. A third phase is also present in some models termed the Interfacial Transition Zone (ITZ) (Zheng & Wei, 2021), see Figure 3-3. The aggregates are distributed randomly in the concrete specimen to form the granular skeleton and the cement paste fills the space between the aggregates. In the model, the matrix depends entirely on the spatial distribution of the aggregates. The digital concrete specimen must be able to be represented in 2D or 3D (although in this project only 2D modelling will be carried out), see Figure 3-2. The shape of the aggregates used in this modelling is circular in 2D plane and spherical in 3D. Although this is not the case in practicality, the impact of the geometry of the aggregate in the model is minimal to the study we are going to be focusing on if we consider results obtained by (Zheng & Wei, 2021) on the matter. It is also possible to model aggregates in a polyhedral shape which is closer to the actual shape of aggregate, see Figure 3-3.

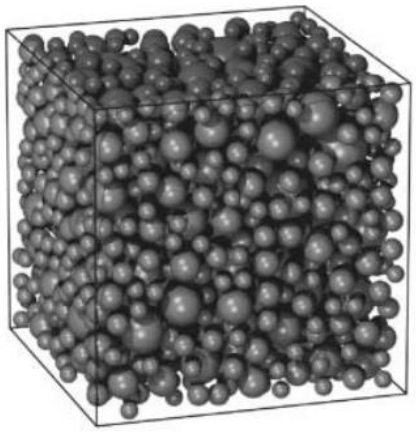

Figure 3-2 (3D) Computer-generated spherical aggregate distribution.

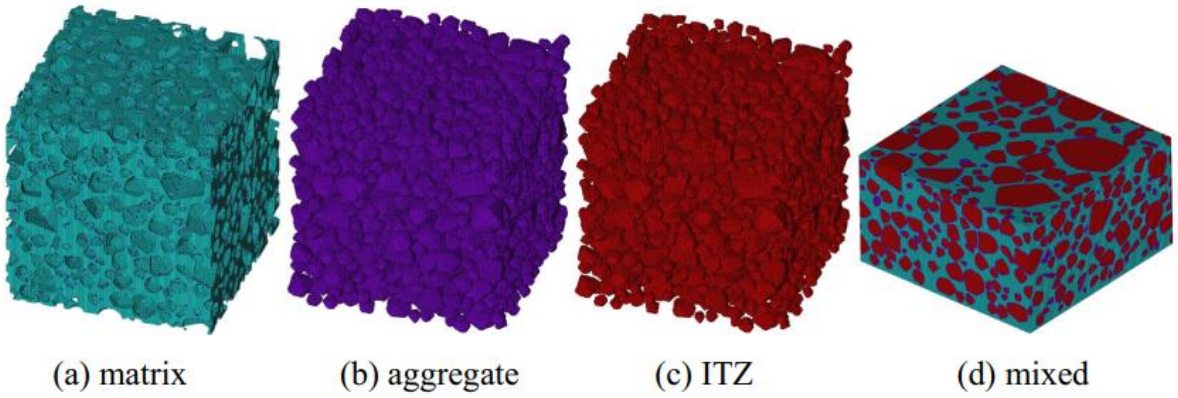

Figure 3-3 Three main phases in the modelling of concrete. (Zheng & Wei, 2021)

3.3 Numerical models.

In order to study the early-age behaviour of massive concrete structures by means of finite element calculations, several models have been proposed. These models facilitate the simulations and represent various parametric conditions in real life. Below is a fair share of finite element models that exist in literature concerning the scope of this study.

3.3.1 Chemo-Thermo-Mechanical Models.

3.3.1.1 Model : (Briffaut et al., 2011)

This model is based on a chemo-thermo-elastic-damage approach with a coupling between creep and damage, although its application is limited to chemo-thermo-mechanical relations in this work.

The evolution of hydration is achieved by the use of a chemical affinity:

$$\dot{\xi} = \tilde{A}(\xi).\exp(\frac{E_a}{RT}) \tag{3.1}$$

where E_a is the activation energy $[J\ mol^{-1}]$, R is the ideal gas constant, T is the temperature $[K]$, ξ is the hydration degree and $\tilde{A}$ (ξ) is the chemical affinity $[s^{-1}]$ given by;

$$\tilde{A}(\xi) = a + b\xi + c\xi^2 + d\xi^3 + e\xi^4 + f\xi^5 + g\xi^6 \tag{3.2}$$

where a, b, c, d, e, f, g are constant material parameters which can be identified from a semi-adiabatic test. For the concrete studied, this polynomial fit gives a better agreement with experimental data. The energy balance equation, which includes the heat release due to hydration reaction, is solved to obtain the temperature evolution:

$$C\dot{T} = \nabla(k\nabla T) + L\dot{\xi} \tag{3.3}$$

in which L is the latent hydration heat $[J\ m^{-3}]$, k is the thermal conductivity $[W\ m^{-1}\ K^{-1}]$ and C is the volumetric heat capacity $[J\ \ m^{-3}K^{-1}]$, which is assumed constant The boundary conditions are assumed to be of convective type. The convective heat flux ϕ $[W\ m^{-2}]$ reads:

$$\phi = h(T_s - T_{ext}) \tag{3.4}$$

where h is the exchange coefficient including convection (after linearization) $[W\ \mathrm{m}^{-2}\mathrm{K}^{-1}]$, $\mathrm{T_s}$ is the temperature on the surface $[K]$ and T_{ext} is the ambient temperature $[K]$ (Briffaut, et al., 2011).

3.3.1.2 Model: (Nguyen et al., 2019)

This model describes the coupled chemo-thermo-mechanical modelling in terms of the phase field.

The thermodynamic equilibrium of a concrete domain under thermal transient is governed by the Fourier's law, which includes the heat release due to hydration reaction:

$$\rho c\dot{T} = \nabla(k\nabla T) + Q_\infty \dot{\alpha} \tag{3.5}$$

where ρc is the volumetric heat capacity, $Q_\infty \dot{\alpha}$ describes the heat release due to hydration reaction, in which $\dot{\alpha}$ is the hydration rate, and Q_∞ represents the potential heat of the hydration reaction, k is the local thermal conductivity matrix influenced by fracture process, and is defined by:

$$k = \left(\xi(g(d)-1)+1\right)k_0 \tag{3.6}$$

in which k_0 is the initial thermal conductivity, $g(d) = (1-d)^2 + \zeta$ is the quadratic degradation function, satisfying $g(0) \approx 1, g(1) \approx 0$ and $g'(1) = 0$. A small parameter $\zeta \ll 1$ is introduced to maintain the well-posedness of the system for partially broken parts of the domain. The parameter ξ is used to describe two situations, $\xi = 0$ for the case where the heat flux is not affected by a crack, and $\xi = 1$ means that no heat will flow through cracks, or cracks are insulating. Considering k_0 is independent from the hydration degree, the associated boundary conditions are as follows:

$$T = \overline{T} \qquad on \qquad \partial\Omega_D \tag{3.7}$$

and

$$n^T(-k\nabla T) = \bar{q} + h(T_s - T_a) \qquad on \qquad \partial\Omega_D \tag{3.8}$$

Ω is an open domain describing a hydration system at time t, containing a crack and Ω_D , Ω_N is its boundary.
where $\overline{T}$ and $\bar{q}$ are respectively the prescribed temperature, heat flux at the boundary Ω_D and Ω_N. T_s , T_a are the body surface and air temperature respectively, h is the convection/radiation. Using Arrhenius law for evolution of heat release due to the hydration process, and by neglecting the effects of mechanical process:

$$Q_\infty \dot{\alpha} = g(d)A_T f(\alpha)e^{\left(\frac{-E_a}{RT}\right)} \tag{3.9}$$

or in another form:

$$\dot{\alpha} = g(d)A_{\alpha}e^{\left(\frac{-E_a}{RT}\right)} \tag{3.10}$$

in which $A_{\alpha} = \frac{A_T}{Q_{\infty}} f(\alpha)$ is identified as the chemical affinity of the hydration reaction.

E_a is the activation energy characterizing the rate of heat generation, R is the ideal gas constant. The parameter AT stands for the ratio of the maximum value of the heat production rate to the latent hydration heat for a normalized definition of the hydration function. The degradation function $g(d)$ is added to ensure that no heat of hydration produced at the cracked area takes place. The chemical affinity function $f\ (\alpha)$, represents the evolution of the normalized heat production rate in terms of the hydration degree.

$$f(\alpha) = \left(\frac{\alpha}{a}\right)^b \left(\frac{1-\alpha}{1-a}\right)^c \tag{3.11}$$

3.3.2 Mechanical damage models.

The chemo-thermo-mechanical models are associated with mechanical damage models to reproduce concrete degradation.

3.3.2.1 Model: (Fichant et al., 1999)

The model was developed by (Fichant et al., 1999)**,** which is based on continuum damage mechanics. The effective stress in the damaged material is related to the macroscopic stress. The relationship between stress and strain tensor is given by:

$$\sigma_{ij} = C_{ijkl}^{damaged}\varepsilon_{kl} \tag{3.12}$$

Where $C_{ijkl}^{damaged}$ is the stiffness of the damaged material, and after substituting elastic strain on the relation total stress-strain, the effective stress $\tilde{\sigma}$ is given by:

$$\tilde{\sigma}_{ij} = C_{ijkl}^{0}\varepsilon_{kl} = C_{ijkl}^{0}\varepsilon_{kl}^{e} + C_{ijkl}^{0}\varepsilon_{kl}^{uco} \tag{3.13}$$

$$or\ \ \tilde{\sigma}_{ij} = C_{ijkl}^{0}(C_{ijkl}^{damaged})_{klmn}^{-1}.\sigma_{mn} \tag{3.14}$$

Where C_{ijkl}^{0} is the initial stiffness tensor. In damage models (for the isotropic version of the model), the relation between total stress σ_{ij} and effective stress $\tilde{\sigma}_{ij}$ is given by the expression below:

$$\sigma_{ij} = (1-d)\tilde{\sigma}_{ij} \tag{3.15}$$

Where d is the damage variable (for the isotropic version d is taken as a scalar). Physically, the variable d is defined as the ratio between micro crack surface and that of the total section material. From (Kachanov, 1986)**,** the damage variable characterises the density

of micro cracks present in an elementary volume of material. This then implies that stress applied to the material is only transmitted by the undamaged part of the total section.

The evolution law of the scalar damage variable is given through the normality rule using the following loading function:

$$f = \varepsilon - \varepsilon_{d0} - \xi \tag{3.16}$$

Where ε_{d0} is the damage threshold. ξ is a hardening/softening variable. The evolution law is written as:

$$d = 1 - \frac{\varepsilon_{d0}}{\varepsilon} \exp(B(\varepsilon_{d0} - \varepsilon)) \tag{3.17}$$

B is a parameter which commands the slope of the softening curve defined by the exponential expression. In its original version, the model couples damage and plasticity.(Matallah et al., 2009)

In a finite element calculation, one can estimate the deformations of the crack width from inelastic constraints.

$$\sigma_{ij}^{in} = \sigma_{ij} - \tilde{\sigma}_{ij} \tag{3.18}$$

The crack opening strain is therefore given by:

$$\varepsilon_{kl}^{uco} = C_{ijkl}^{-1} . \sigma_{ij}^{in} \tag{3.19}$$

3.3.2.2 Model: (Mazars, 1984)

The particularity of this model is its use of strain criteria by the introducing the concept of equivalent strain. The model takes into account the asymmetry of the behavior of concrete. However, this model does not take into account other related phenomena linked to the behavior of concrete such as irreversibility of deformation, anisotropy and the unilateral effect. The model is as follows.

For a given state of damage D, the evolution threshold and equivalent deformation is expressed by:

$$\tilde{\varepsilon} = \sqrt{\langle \varepsilon_1 \rangle_+^2 + \langle \varepsilon_2 \rangle_+^2 + \langle \varepsilon_3 \rangle_+^2} \tag{3.20}$$

Where ε_i is the principal deformation in the direction i and $\langle \ \rangle_+$: indicates Mac Cauley's sign.

the threshold surface is expressed as follows:

$$f(\varepsilon, D) = \varepsilon - K(D) = 0 \tag{3.21}$$

Where $K\ (0)\ =\ \varepsilon_{d0}$ corresponds to the damage threshold of fresh material.

The evolution of D satisfying the Clausius-Duhem inequality ($-Y\dot{D} > 0$), which leads to an integrated form.

$$D = F(\varepsilon) \tag{3.22}$$

with: $F(\varepsilon)$ a positive continuous function of ε.
For the asymmetric behavior of concrete, Mazars offers two damage models, D_t for traction and D_c for compression. The linear combination of these two damages gives the global isotropic damage:

$$D = \alpha_t.D_t + \alpha_c.D_c \qquad and \qquad \alpha_t + \alpha_c = 1 \tag{3.23}$$

The coefficients α_t and α_c represent the coupling of tensile-damage and compression-damage respectively. In pure traction $\alpha_t = 1, \alpha_c = 0$ and in pure compression $\alpha_t = 0$, $\alpha_c = 1$.

The evolution of D_t and D_c is of the form:

$$D_i(\varepsilon) = 1 - \frac{K(0)(1-A_i)}{\varepsilon} - \frac{A_i}{\exp\left[B_i(\varepsilon - K(0))\right]} \tag{3.24}$$

With $i = t\ or\ c$; A_t, B_t, A_c, B_c are characteristic parameters of the model.

This model does not take into consideration permanent deformations or the unilateral effect. Taking a constant value of $\alpha_t$constant limits the scope of the model and the introduction of the equivalent deformation expression (3.20) leads to a strict condition where damage is produced only if there is at least one extension in the main deformation coordinate system. (Ghezali, 2012)

3.3.3 Crack opening Estimation. (Matallah et al., 2009)

The model adopted for calculating crack openings in a concrete structure is a continuous modeling approach based on damage mechanics. A post-processing method based on energy regularization to extract crack openings from a continuous damage calculation in finite elements models was proposed by (Matallah et al., 2009). This method is applicable to all continuous damage and/or plasticity models.

In models based on continuous approaches, it is assumed that the crack is located in a band of width, h, and the micro cracks are considered to be uniformly distributed. The energy dissipation is constant, and given by the following formula:

$$G_f = \int_0^{\infty} \sigma d\delta \tag{3.25}$$

Where: δ : crack opening displacement.
The crack opening displacement is calculated as the product of breaking strain ε^{uco} and the width of the band h.

$$\delta = \varepsilon^{uco}.h \tag{3.26}$$

Where we consider ε^{uco}as the Unitary Crack Opening (UCO) strain variable (fracture strain). The total strain in the fracture zone consists of an elastic portion and a fracture portion. So, the fracture energy per unit width is calculated as the area under the complete stress-strain diagram:

$$G_f = \int_0^{\infty} \sigma d\varepsilon^{uco} = h\int_0^{\infty} \sigma d\varepsilon \tag{3.27}$$

3.3.3.1 Fracture energy within a damage finite element computation

If we consider now the damage model presented above, the constitutive law is given by:

$$\sigma_{ij} = (1-d)C_{ijkl}\varepsilon_{kl} \tag{3.28}$$

And subsequently, substituting for expression (3.17) and the general expression of $\sigma = E\varepsilon$:

$$G_f = h\int_0^{\infty} E(1-d)\varepsilon d\varepsilon = h\int_0^{\infty} E\frac{\varepsilon_{d0}}{\varepsilon}\exp(B(\varepsilon_{d0}-\varepsilon))\varepsilon d\varepsilon = h\left(\frac{\varepsilon_{do}^2}{2}+\frac{\varepsilon_{do}^2}{B}\right) \tag{3.29}$$

In the failure zone, the total deformation strain is defined as the sum of the total elastic and inelastic strain deformations, given by the expression below:

$$\varepsilon_{ij} = \varepsilon_{ij}^{e} + \varepsilon_{ij}^{uco} \tag{3.30}$$

The total strain is decomposed into two parts: an elastic part $\varepsilon^{e}$and a cracking part represented by the UCO strain variable ε^{uco}. Multiplying (3.30) by the elastic stiffness tensor C_{ijkl}, we obtain:

$$\tilde{\sigma} = C_{ijkl}\varepsilon_{kl} = C_{ijkl}\varepsilon_{kl}^{e} + C_{ijkl}\varepsilon_{kl}^{uco} = \sigma_{ij} + \sigma_{ij}^{in} \tag{3.31}$$

Thus, the tensor of the crack openings strain is given by:

$$\varepsilon_{ij}^{uco} = C_{ijkl}^{-1}\sigma_{ij}^{in} \tag{3.32}$$

And from a finite element computation, we get a total stress σ, the effective stress is computed using the total strain equation (3.14). The inelastic stress tensor is therefore given by:

$$\sigma_{ij}^{in} = \sigma_{ij} - \tilde{\sigma}_{ij} \tag{3.33}$$

Equation (3.32) gives the UCO strain tensor. The normal crack opening displacement value is given by:

$$\delta_n = n_i \delta_{ij} n_j = n_i h \varepsilon_{ij}^{uco} n_j \tag{3.34}$$

Where n is the unit vector normal to the crack. For a one-dimensional test:

$$\delta_n = h \varepsilon_{nn}^{uco} \tag{3.35}$$

3.4 Adopted Models.

For the purpose of this study, we have chosen to work with models from (Briffaut et al., 2011) for chemo-thermo-mechanical modelling. A damage model using (Fichant et al., 1999) and we are going to employ the procedure for crack estimation from (Matallah et al., 2009).

3.5 Parameters being evaluated.

The purpose of these models is to evaluate the stress, damage and crack opening evolutions in early age concrete. The study goes on to further evaluate the mechanical behaviour and the effect of dimensions on early age concrete.

3.5.1 Boundary conditions.

A $(20 \times 20) cm^2$ sample will be used following the boundary conditions illustrated in Figure 3-4. In addition, a $(10 \times 10) cm^2$ sample will also be used for a study on the effect of dimensions using the same boundary conditions illustrated below.

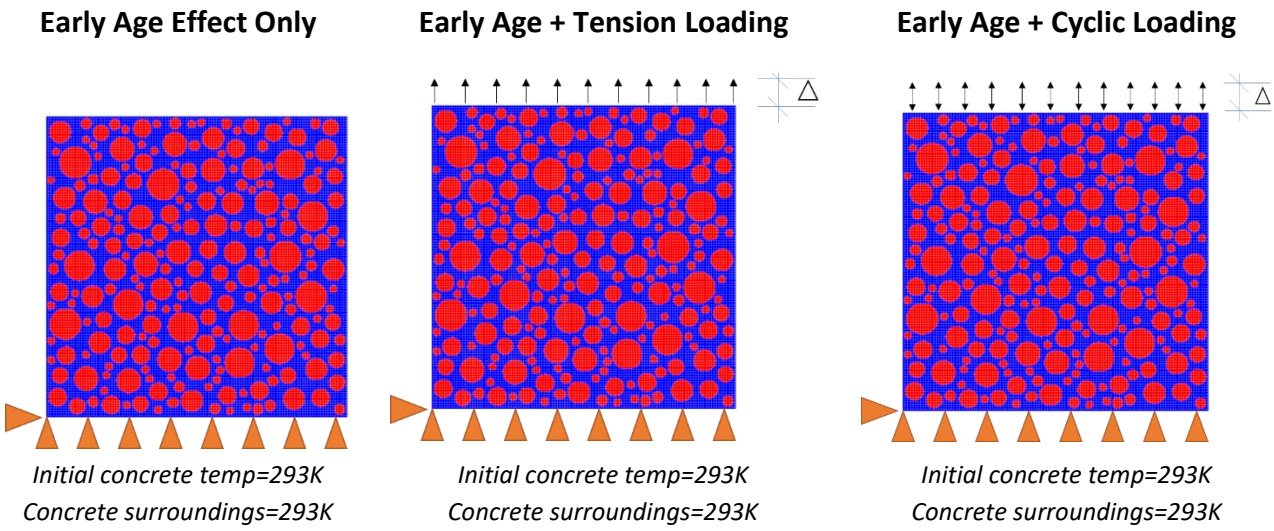

Figure 3-4 Boundary conditions.

3.5.2 Constants and coefficients.

Table 3-1 Mechanical characteristics of paste and aggregates.

	$E(GPa)$	ϑ	$f_t(MPa)$	$G_f(J/m^2)$
Mortar	15	0.2	3	20
Coarse aggregate	60	0.2	6	60

Table 3-2 Other parametric values used in the simulations

Parameter	Value	Units
Volumetric mass	2500	kg/m^3
Volumetric heat capacity	2400	$kJ/°C.m^3$
Thermal conductivity of concrete	2.6	$W/K.m$
Activation energy	45729.75	J/mol
Gas constant	8.3145	$J/K.mol$
Convection coefficient	12.5	$W/K.m^2$
Latent heat of hydration	117840	$kJ.m^3$
Chemical affinity	1.2	s^{-1}

Thermal coefficient	7.5	$\mu m/m.℃$
Final endogenous shrinkage	40	$\mu m/m$
a	64.417	
b	18042	
c	-94620	
d	215819	
e	-280339	
f	208172	
g	-67901	
Ambient room temperature	293	K

In this chapter, the granular class composition used is shown in Table 3-3,

Table 3-3 Volume fraction of each granular class

5/7 ; 7/16 ; 16/21	
Diameter (mm)	**Volumetric %**
21	4
20	6
16	6
14.5	8
12	8
10,5	6
7	4
5	4

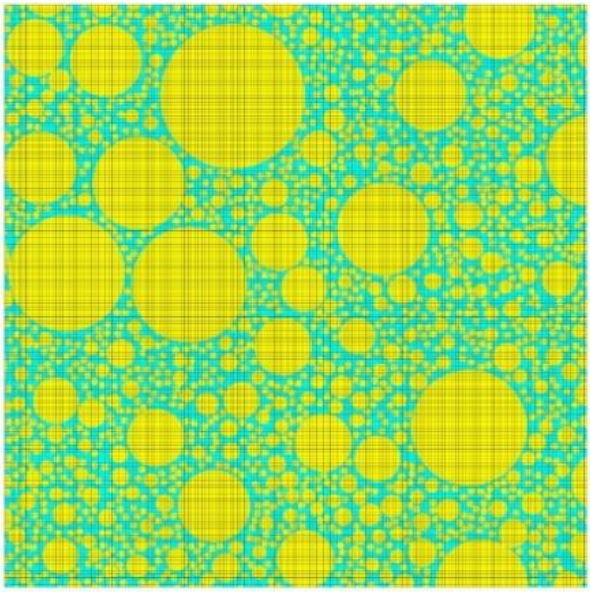

$(10 \times 10)cm^2$

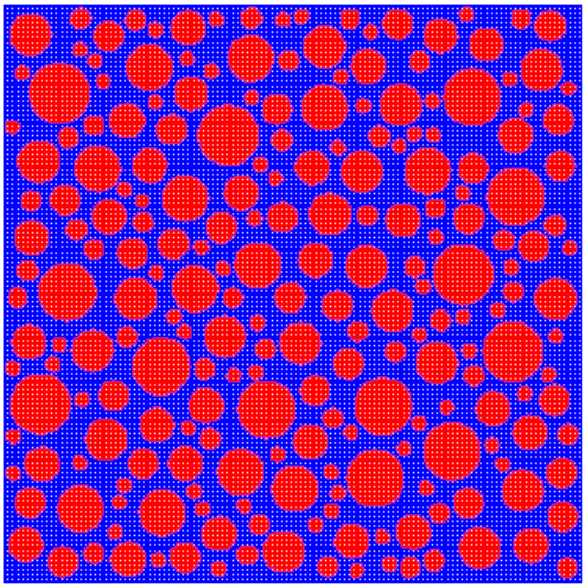

$(20 \times 20)cm^2$

Figure 3-5 Meshing of concrete and granular distribution.

3.6 Results and analysis for $(\mathbf{20} \times \mathbf{20})\boldsymbol{cm}^{\mathbf{2}}$ model.

3.6.1 Effect of Early Age on concrete.

With Early Age | **Without Early Age**

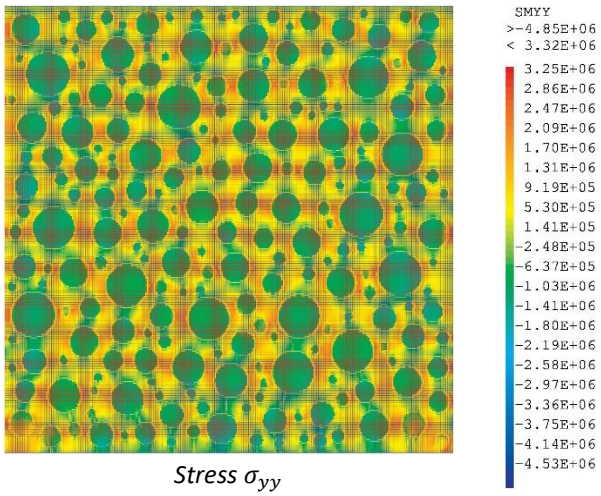

Stress σ_{yy}

No stresses

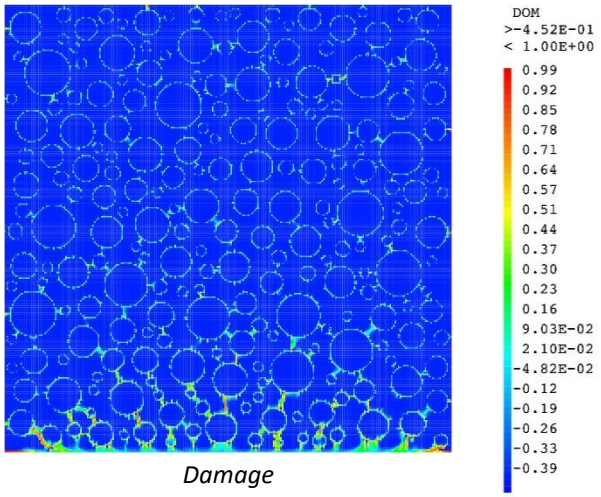

Damage

No Damage

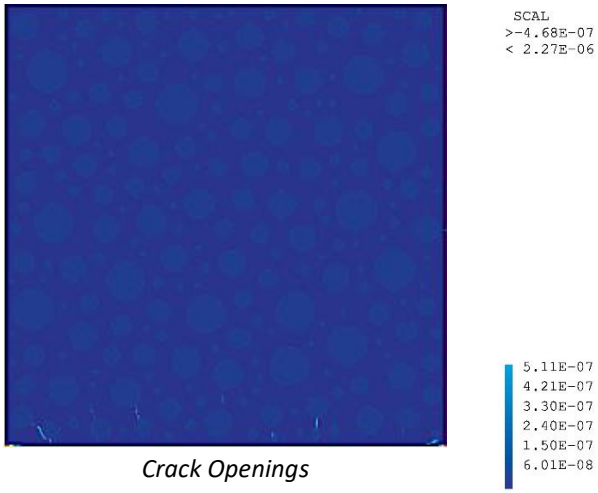

Crack Openings

No Crack Openings

Figure 3-6 Stress, damage and crack openings due to early age only.

3.6.2 Effect of Early Age under Tension loading.

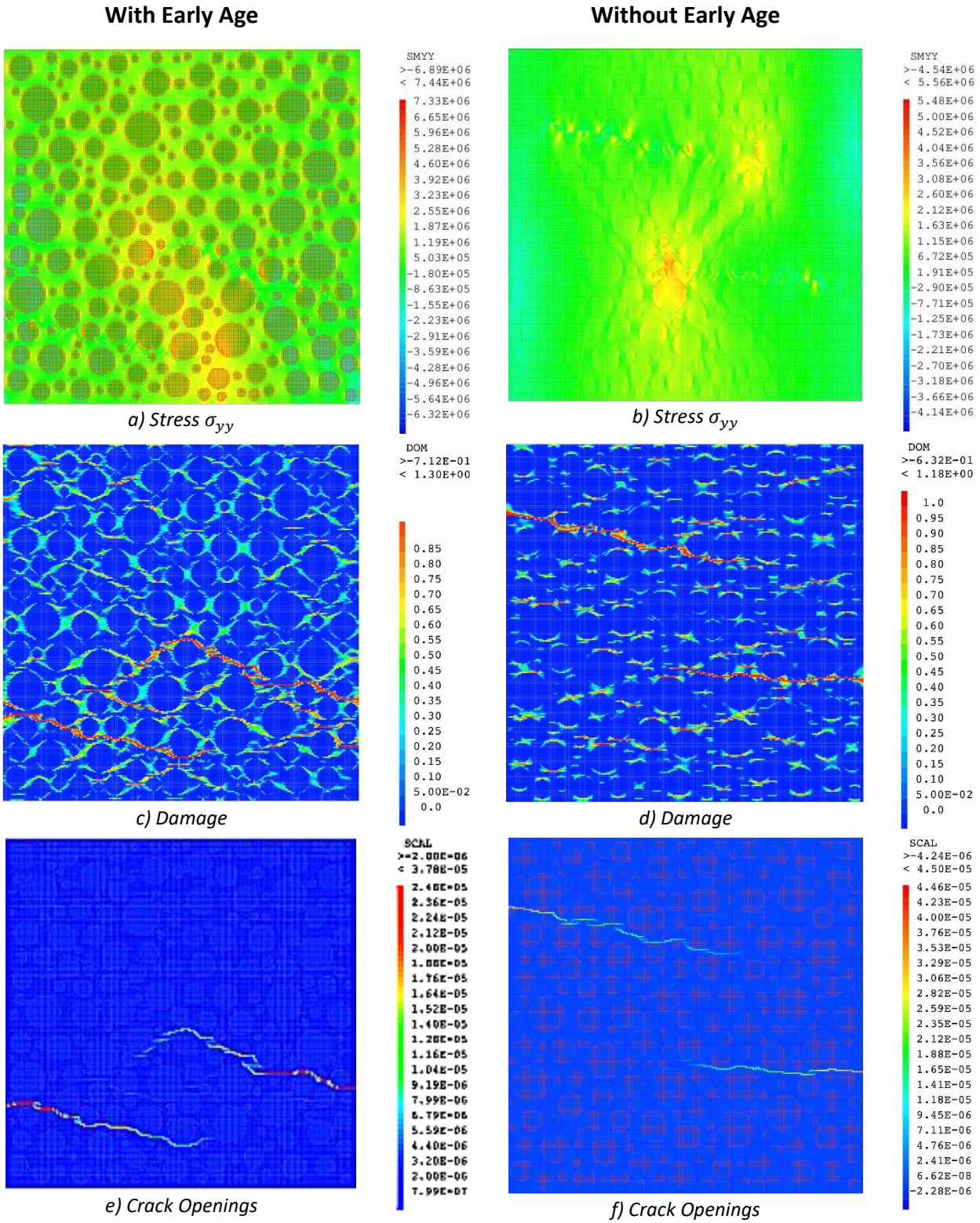

Figure 3-7 Stress, damage and crack openings due to early age under tension loading.

Figure 3-6 shows stress, damage and crack openings for concrete with early age hydration (EA concrete). It is important to note that concrete without early age (WEA concrete) does not have any stresses, damage or crack openings. Going on to the nature of distribution of the stress, damage and crack openings, they are all orthogonal to the boundary conditions defined in Figure 3-4. This further solidified (2.3.1.2) and affirms that restraints are a primary cause of cracking in early age concrete.

A maximum crack opening of $2.14296 \times 10^{-6}m$ developed due to early age hydration only. According to (ACI, 2017) the maximum allowable crack width limit in concrete exposed to dry air is $4.1 \times 10^{-4}m$, which is incomparably greater than the maximum figure obtained from the simulations.

Figure 3-7 shows the stress, damage and crack opening evolution of EA concrete and WEA concrete. A more significant damage density is witnessed on EA concrete (visual comparison between (c) and (d)). The crack openings of both samples are produced following the densest damage paths and occur on the concrete paste. For the WEA concrete, all primary crack and damage seams are at an almost perfect perpendicular direction to the loading plan (Oy), whereas the ones from the EA concrete are angled, confirming the existence of primary stresses independent and of the loading component provoking the primary cracking.

3.6.2.1 Global mechanical behaviour under tension.

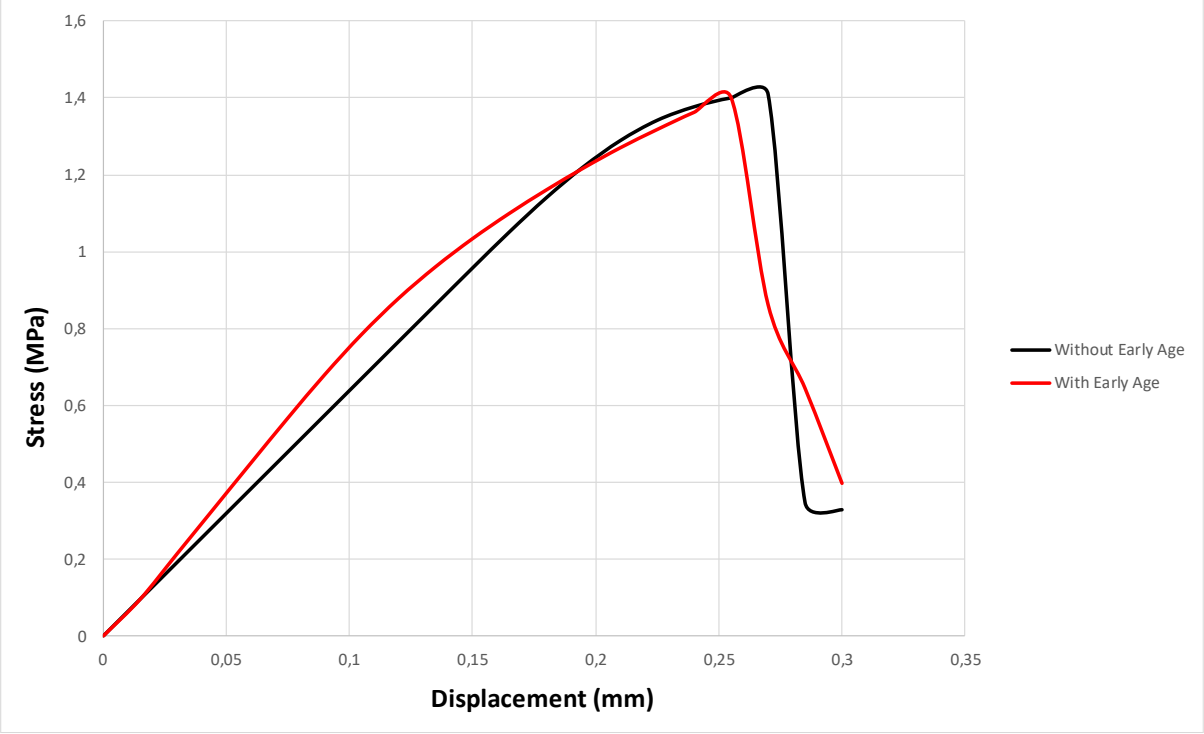

Figure 3-8 Global mechanical behaviour of EA and WEA concrete under tension loading.

Figure 3-8 shows stress- displacement evolution of EA and WEA concrete under tension. WEA concrete shows a marginally superior maximum stress capacity.

3.6.3 Effect of Early Age under cyclic loading.

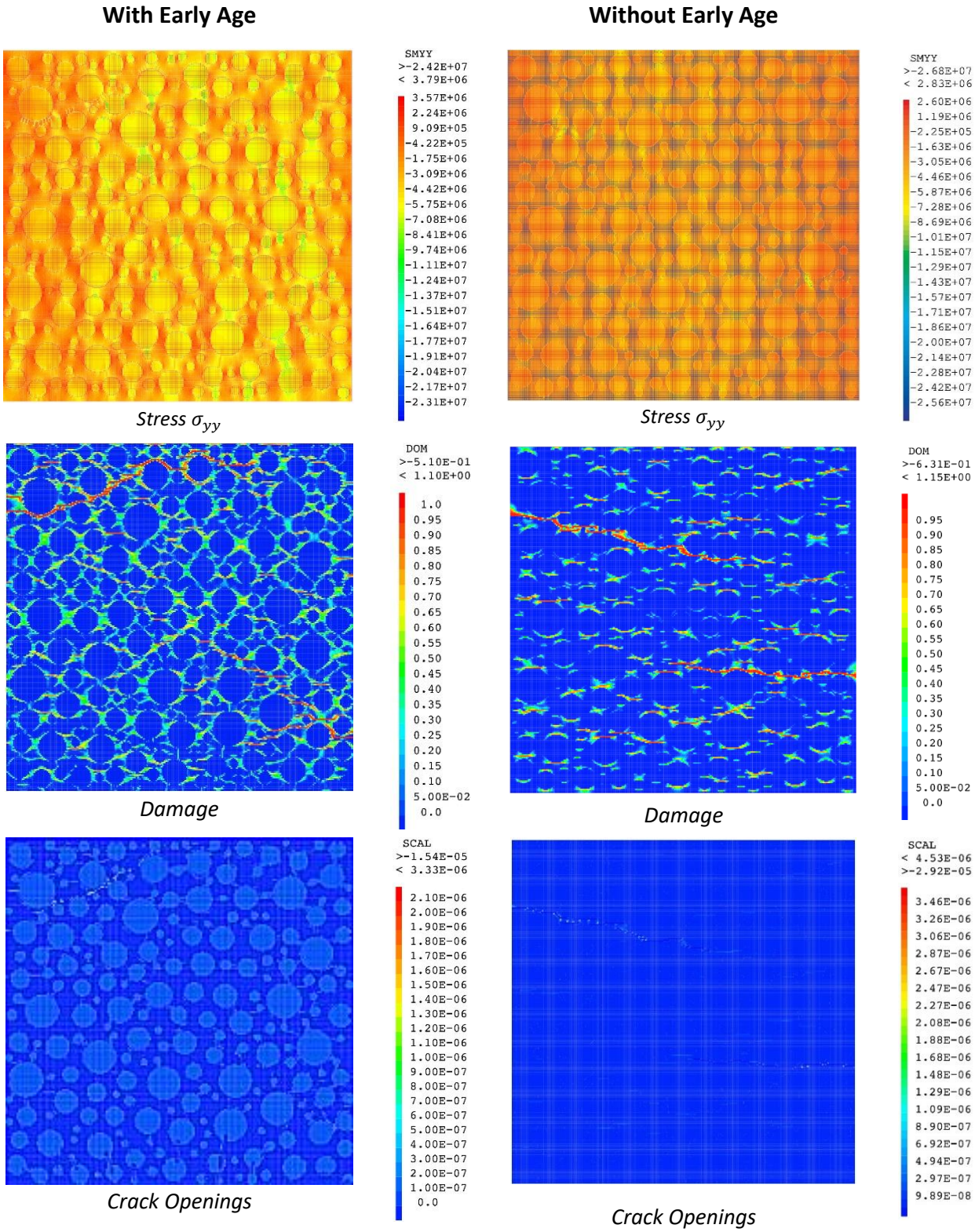

Figure 3-9 Stress, damage and crack openings due to early age under cyclic loading.

Figure 3-9 shows the distribution of stresses, damage and crack openings due to cyclic loading of EA and WEA concrete. Looking on from Figure 3-7, there's a significant decrease in the damage density distribution and crack openings. This is all because of seam reclosing due to an imposed compressive strain in the cyclic loading regime.

3.6.3.1 Global mechanical behaviour under cyclic loading.

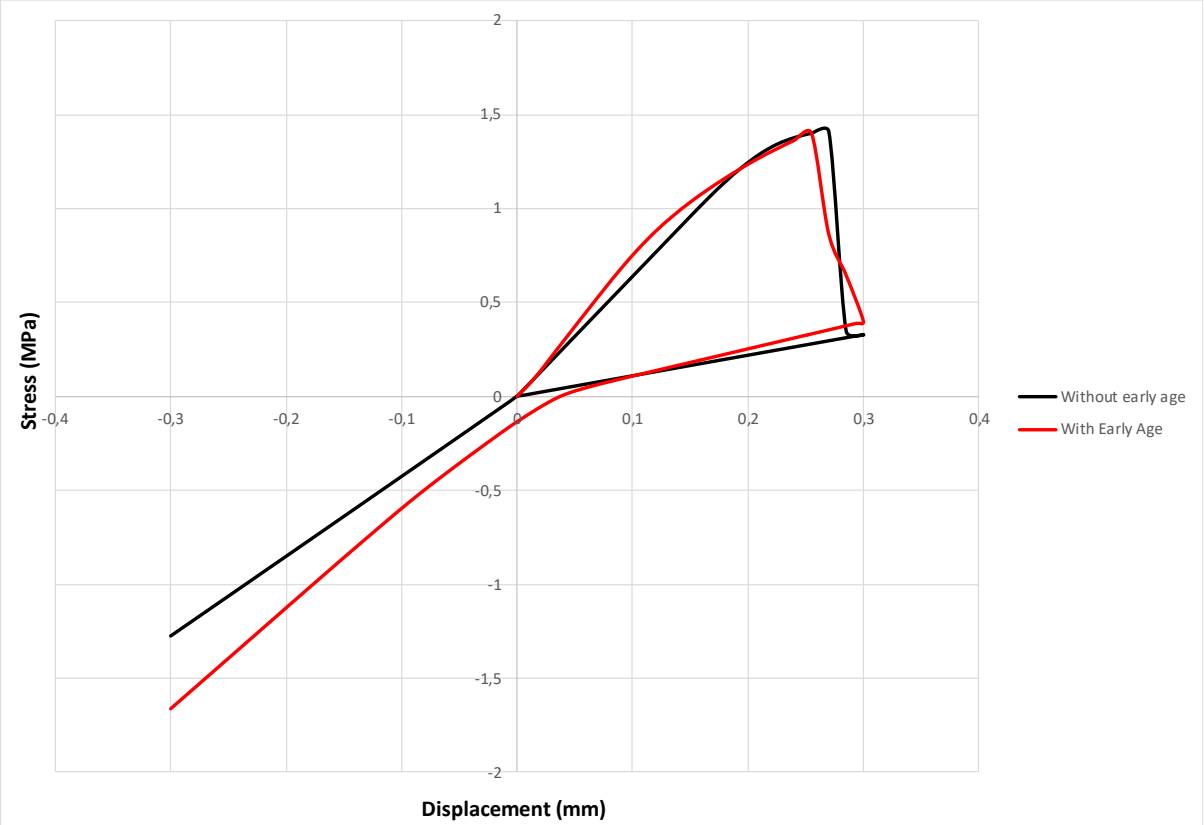

Figure 3-10 Global behavior of concrete under cyclic loading.

Figure 3-10 depicts that the initial stress state due to the hydration process plays an important role. The value of the seam reclosing stress is greatly modified. A negative value is obtained instead of a perfect strain recovery as portrayed by a concrete sample without early age hydration. This is consistent with literature findings from (La Borderie et al., 2010; NGuyen, 2010), and implies that the concrete with early age hydration experiences permanent deformation with every cycle of loading. Negative stress deformation is relatively constant for both samples. The behaviour at early age computed is considered as an initial state (stresses, internal variables, displacements).

3.6.4 Evaluation of the effect of dimensions on the Hydration Temperature evolution in Concrete.

Two concrete specimens of different dimensions, $(10 \times 10)cm^2$ and, $(20 \times 20)cm^2$ were simulated with early age to analyse the effects of geometry or dimensions on the maximum hydration temperature in concrete. Figure 3-11 shows the temperature evolution of the 2 samples.

3.6.4.1 Temperature evolution.

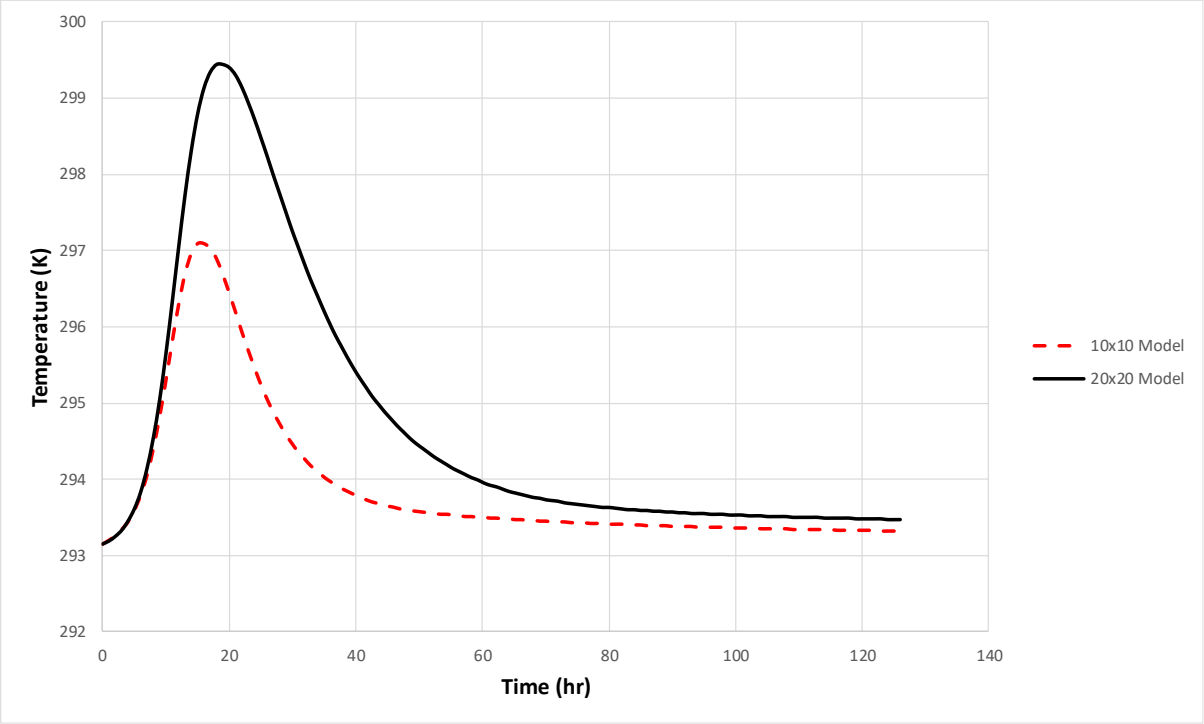

Figure 3-11 Hydration temperature evolution of a $(10 \times 10)cm^2$ *model and a* $(20 \times 20)cm^2$

As observed from Figure 3-11, a lower peak and a favourable thermal evolution in the $(10 \times 10)\text{cm}^2$ sample is witnessed as compared to the $(20 \times 20)\text{cm}^2$ one. These observations further demonstrate the vulnerability of massive structures with respect to early age hydration. It also affirms the effectiveness of phase casting in limiting the maximum hydration temperature in massive structure constructions.

3.6.5 Validation of model findings.

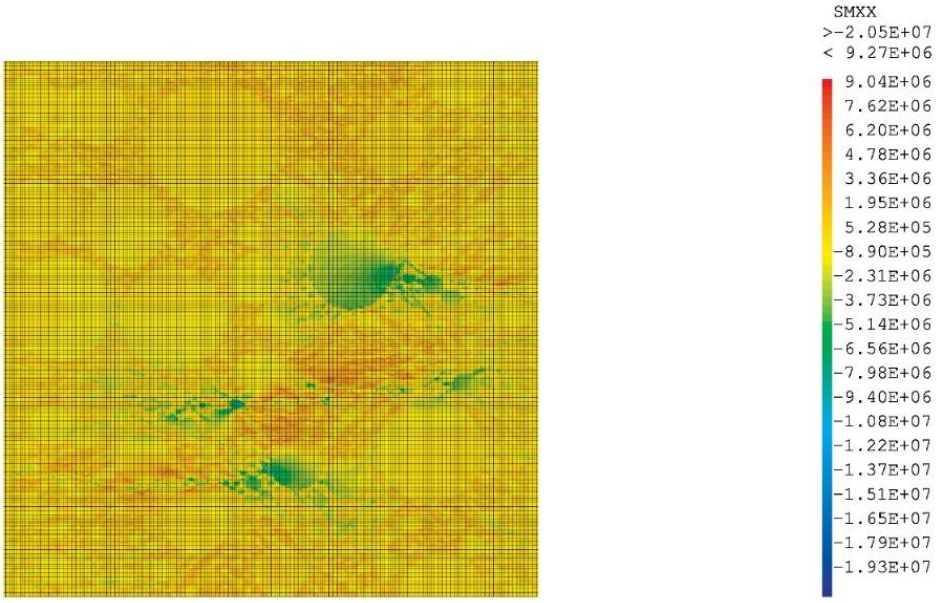

Figure 3-12 Stress evolution of a $(10 \times 10)cm^2$ *model after cyclic loading.* σ_{xx}

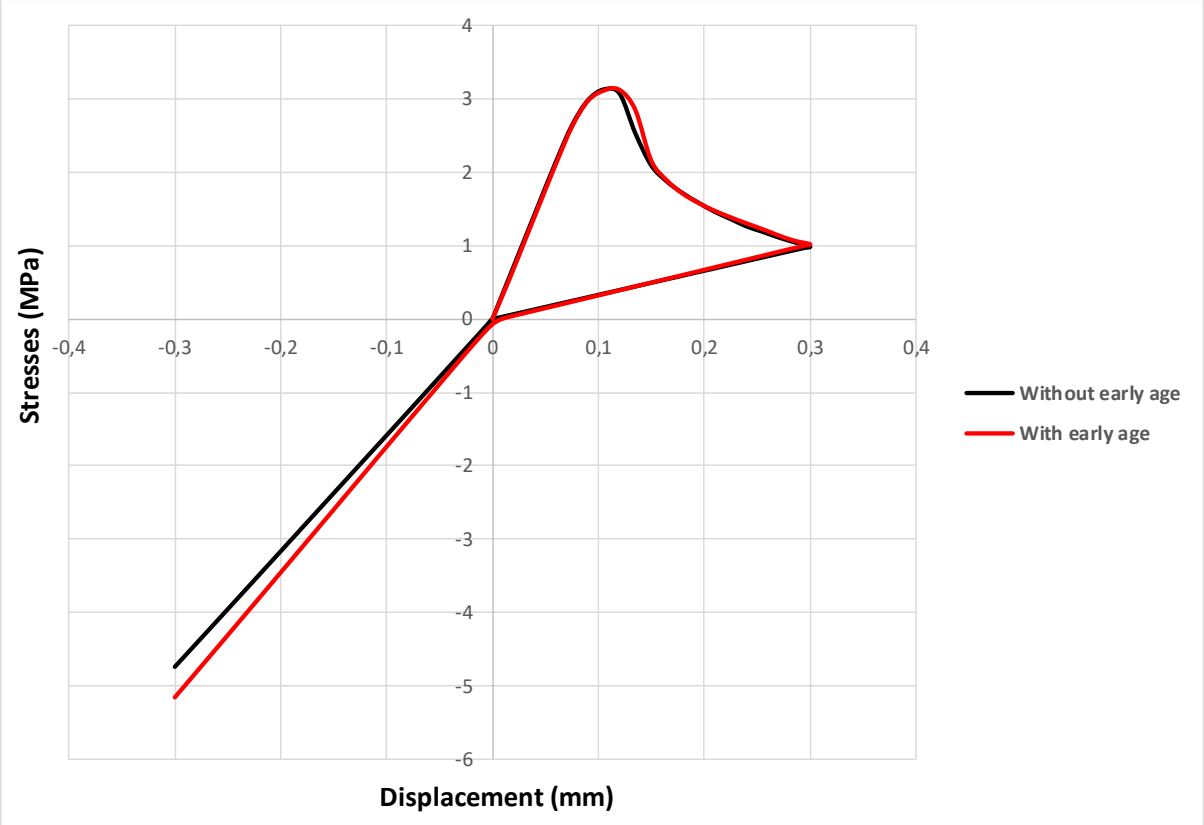

Figure 3-13 Global behavior of concrete under cyclic loading. $(10 \times 10)cm^2$ *model*

The findings herein, Figure 3-12 and Figure 3-13, are in agreement with those by (NGuyen, 2010) using the same simulations parameters.

3.7 Conclusion.

A numerical chemo-thermo-mechanical procedure has been presented in this chapter. Based on experimental observations, we find that the behavior of concrete is greatly influenced by early age hydration. The existence of initial stresses due to the hydration process play an important role. The value of the seam reclosing constraint in cyclic loading is modified. A negative value is obtained instead of the classical value imposed by the damage model without early age hydration ($\sigma = 0$). Although the extent of this effect was found to be minimal in these models, it is important to note that evidence of the effect of dimensions on early age concrete was affirmative. This then validates the effect of early age hydration in massive structures.

Chapter 4: Numerical analysis of Temperature control in concrete.

4.1 Introduction.

In this chapter, we examine the effectiveness of various precooling and post cooling methods. This is made possible by the use of mesoscopic models defined in the preceding chapter. A comparison of aggregate and pipe cooling methods will be undertaken with respect to damage and crack evolutions after early age hydration, tension loading and cyclic loading. The global stress evolution will also be analysed for both tension and cyclic loading to see the overall mechanical behaviour of concrete under the 2 cooling methods.

4.2 Additional Parameters.

To analyse the effect of different granular class compositions used in aggregate cooling, a second granular class composition was used for comparative purposes, see Table 4-1.

Table 4-1 Different granular class composition.

$5/7$; $7/16$; $16/21$		$5/8$; $8/16$; $16/25$	
Diameter (mm)	**Diameter (mm)**	**Diameter (mm)**	**Volumetric %**
21	21	25	8.59
20	20	20	10.96
16	16	16	6.56
14.5	14.5	12.5	6.76
12	12	10	5.72
10,5	10,5	8	2.96
7	7	6.3	1.65
5	5	5	1.66

Figure 4-1 shows the meshing of the pipe cooling model and the meshing of the second granular class composition model.

Table 4-2 shows the main characteristics of the 2D cooling pipe method used and Table 4-3 shows the initial temperatures of aggregates and cement paste for the pipe cooling method.

Table 4-2 Model parameters for the cooling pipes

Characteristics of the cooling pipe system	**Values**
The coefficient of convective heat transfer on the pipe loop, $W/m^2\ °C$	282
Speed, m/s	0.5
Water temperatures in the pipes, $°C$	293
The density of water, kg/m	1000
Specific heat capacity, $kJ/(kg\ °C)$	1.12
Thermal conductivity, $W/(m\ °C)$	0.64
Pipe radius, m	0.003
The duration of cooling	127hrs
Ambient temperature (K)	293

Table 4-3 Initial temperatures for aggregate cooling method.

	Initial Temperature (K)
Aggregates	283
Cement paste	293

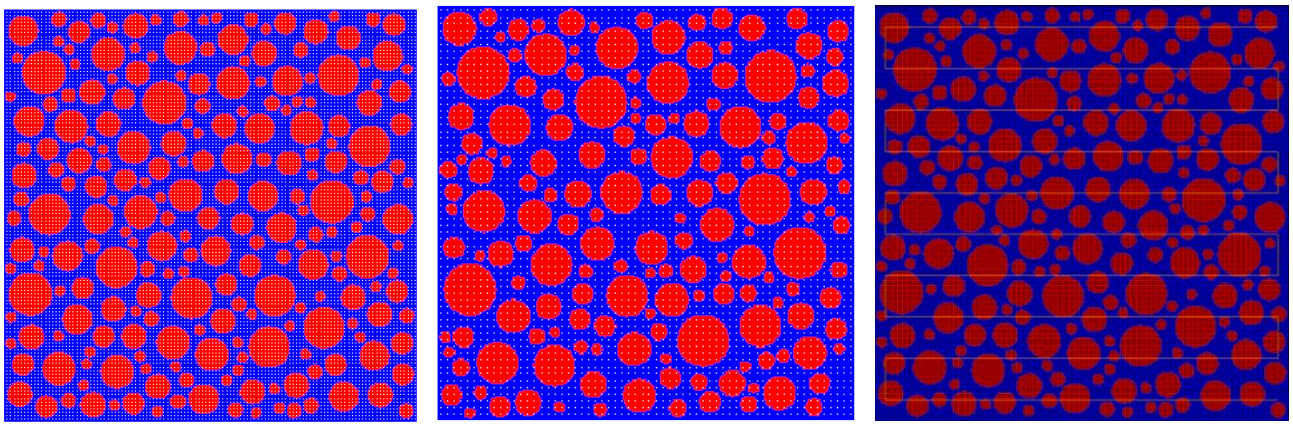

Granular composition: 5/7 ; 7/16 ; 16/21

Granular composition: 5/8 ; 8/16 ; 16/25

Pipe Cooling

Figure 4-1 Meshing

4.3 Results and analysis for $(\mathbf{20 \times 20})\boldsymbol{cm^2}$ model.

4.3.1 Effect of Aggregate Cooling and Pipe Cooling on Early Age Concrete.

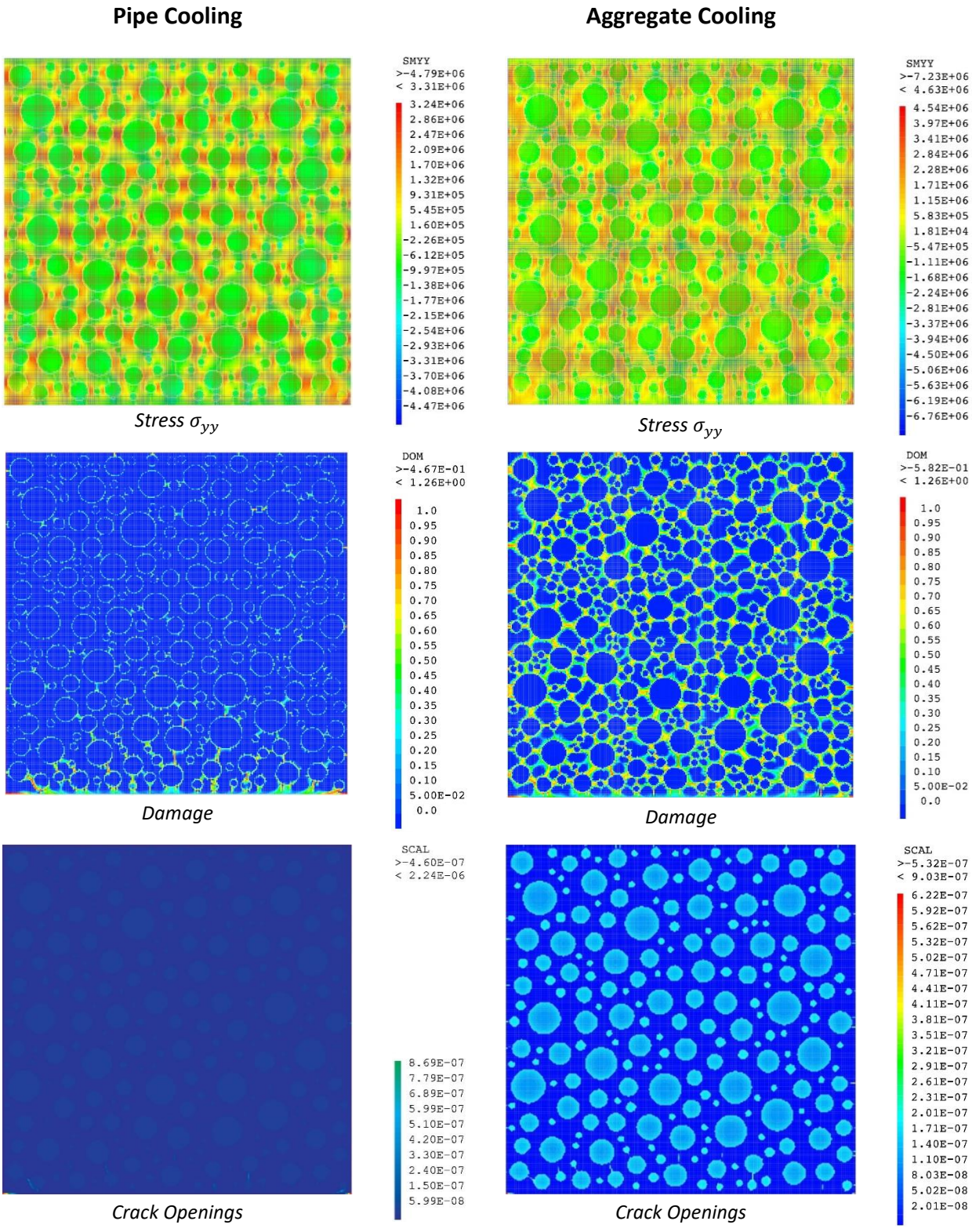

Figure 4-2 Stress, damage and crack openings due to early age only.(Aggregate and pipe cooled)

4.3.1.1 Temperature evolution.

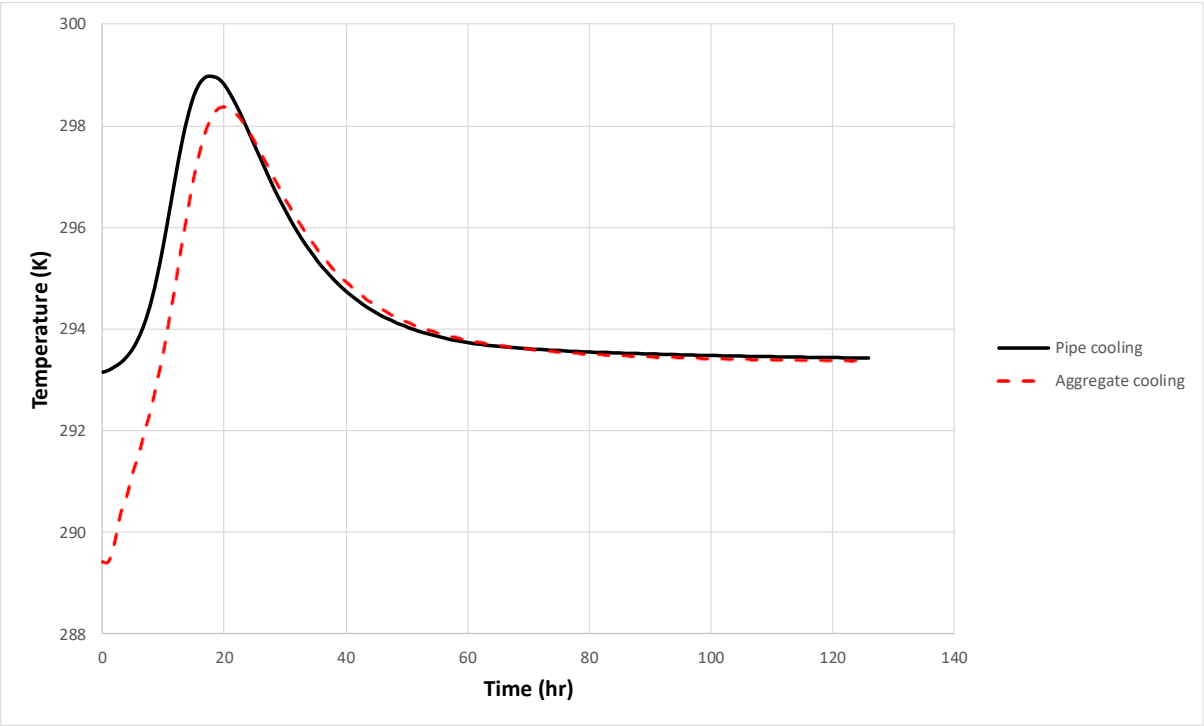

Figure 4-3 Hydration temperature evolution of an aggregate cooled model and a pipe cooled model.

Figure 4-2 shows stresses, damage and crack openings of aggregate and pipe cooled concrete samples due to early age hydration only. As observed, all the damage and crack openings developed are orthogonal to the boundary conditions defined in (3.5.1) and as stated in (2.3.1.2).

Figure 4-3 demonstrates that aggregate cooling method has a relatively lower initial and peak temperatures as compared to pipe cooling. The thermal evolution is almost comparable though better for pipe cooling with relation to initial and final temperature fluctuations.

4.3.2 Effect of Aggregate Cooling and Pipe Cooling on Early Age Concrete subjected to tension loading.

Pipe Cooling **Aggregate Cooling**

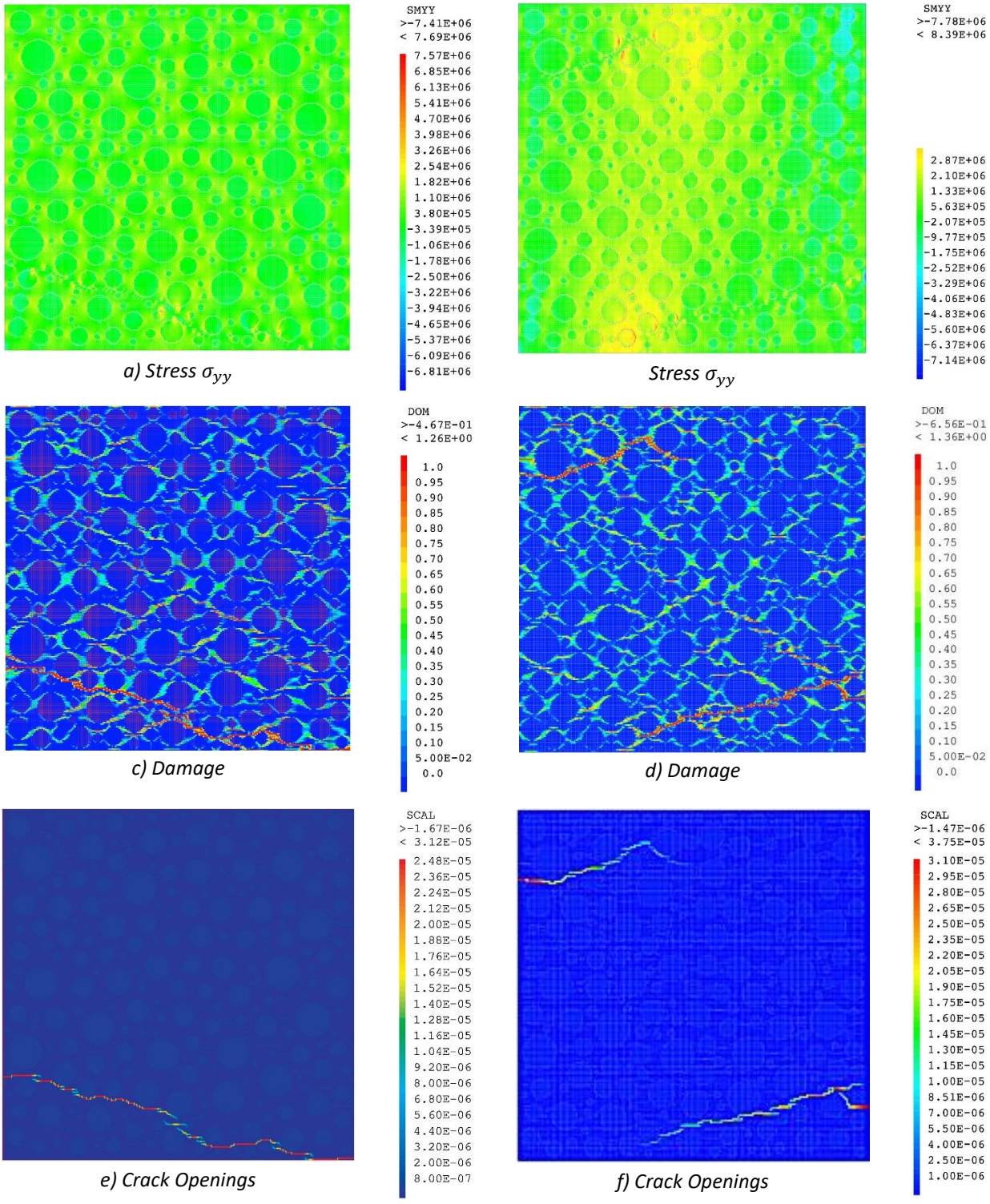

a) Stress σ_{yy} *Stress σ_{yy}*

c) Damage *d) Damage*

e) Crack Openings *f) Crack Openings*

Figure 4-4 Stress, damage and crack openings due to early age and under tension. (Aggregate and pipe cooled)

4.3.2.1 Global mechanical behaviour under tension.

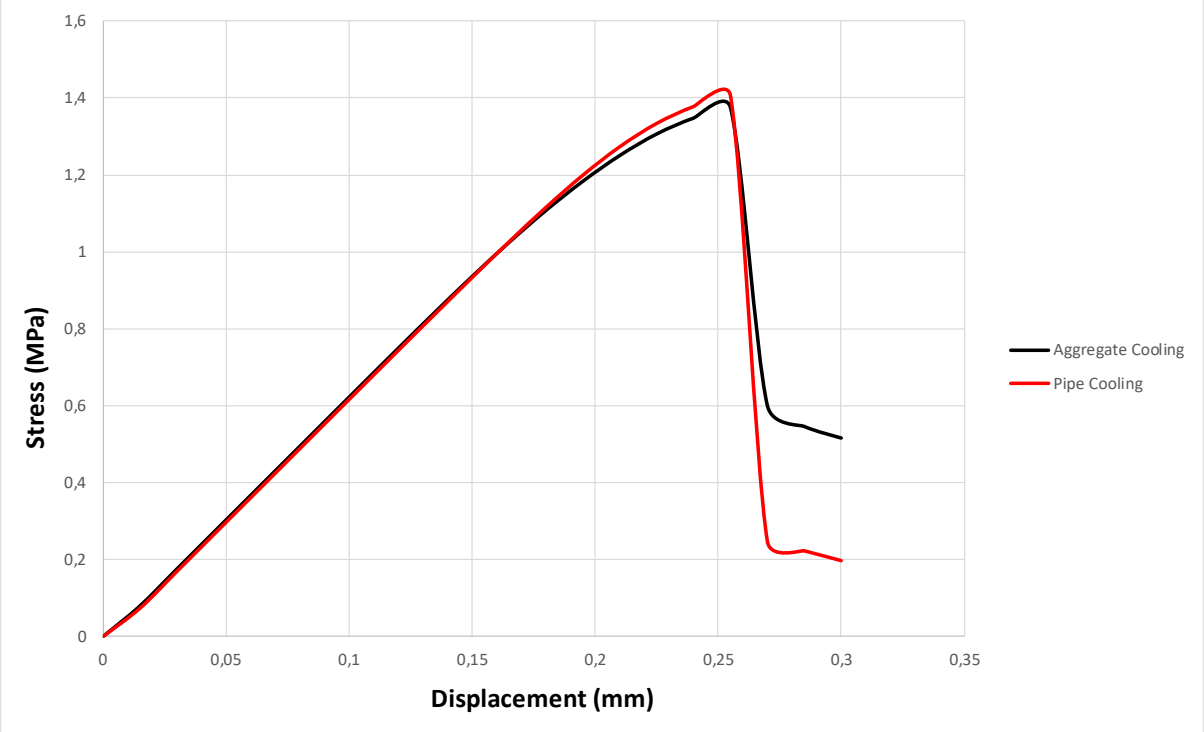

Figure 4-5 Global mechanical behaviour of pipe and aggregate cooled concrete samples under tension.

Figure 4-4 illustrate the evolution of damage and crack openings. The damage density distributions are almost uniform for the two samples (c and d) although two primary seams developed for the aggregate cooled sample.

Figure 4-5 shows the global behaviour of pipe and aggregate cooled early age concrete. Both samples portray a brittle behaviour. The pipe cooled sample also has a slightly higher maximum stress implying better mechanical behaviour although the difference is minute.

4.3.3 Effect of Aggregate Cooling and Pipe Cooling on Early Age Concrete subjected to cyclic loading.

Pipe Cooling **Aggregate Cooling**

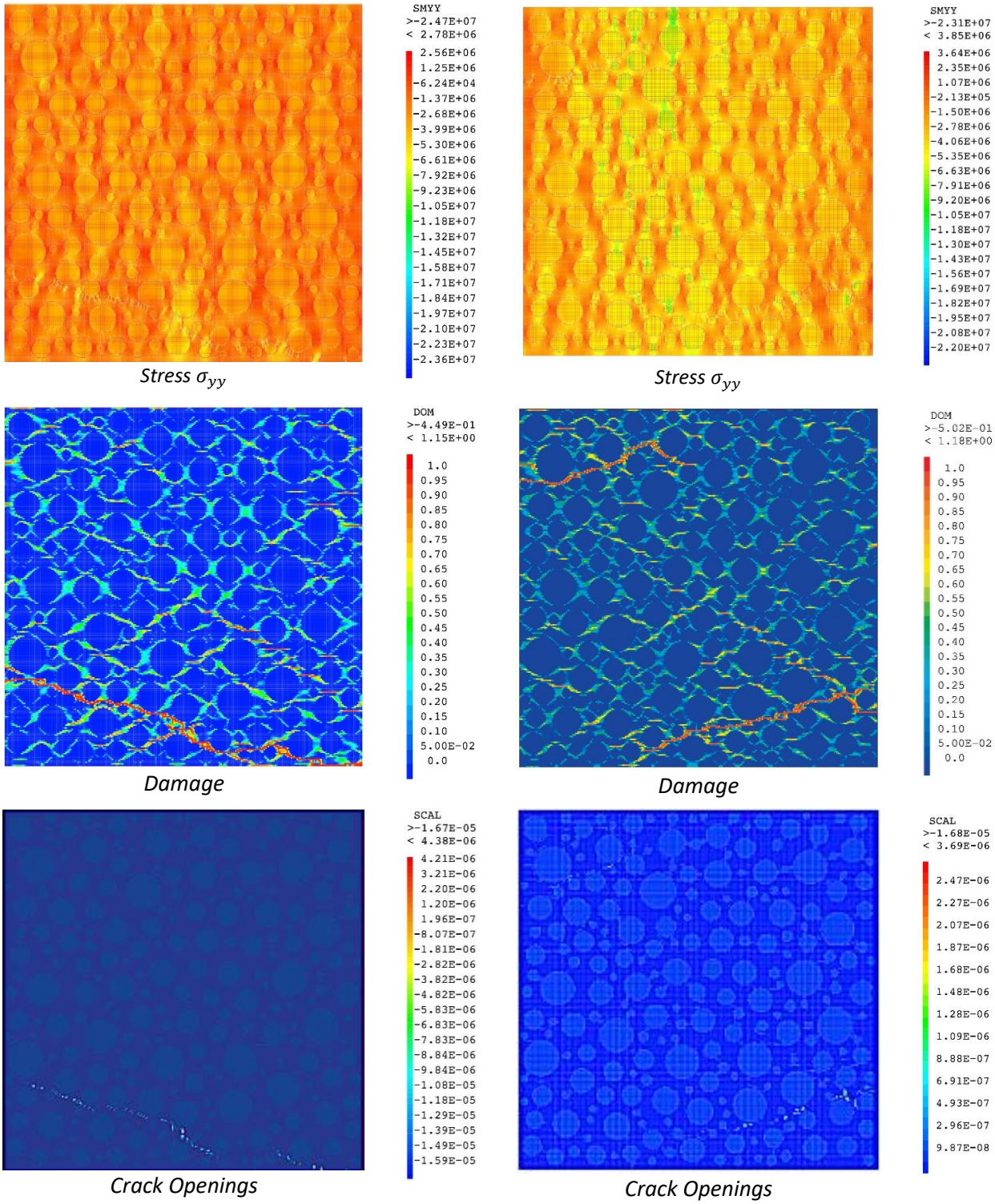

Stress σ_{yy} *Stress σ_{yy}*

Damage *Damage*

Crack Openings *Crack Openings*

Figure 4-6 Stress, damage and crack openings due to early age under cyclic loading. (Aggregate and pipe cooled)

Figure 4-6 shows the distribution of stresses, damage and crack openings of an aggregate and pipe cooled model under cyclic loading.

4.3.3.1 Global mechanical behaviour under cyclic loading.

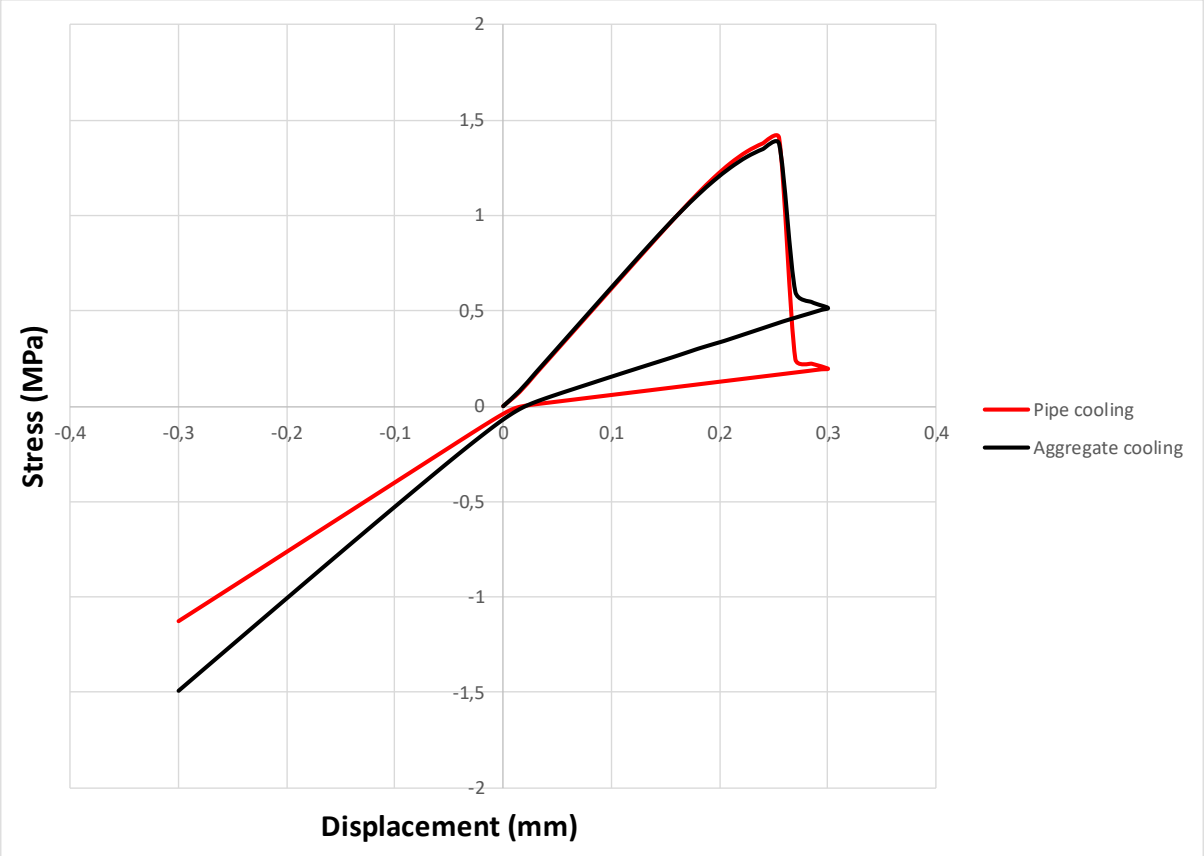

Figure 4-7 Global behavior of concrete under cyclic loading. (Aggregate and Pipe cooled)

Figure 4-7 shows stress evolution of an aggregate and pipe cooled sample. A slightly improved negative seam reclosing strain is witnessed with the pipe cooling method.

4.3.4 Global temperature and mechanical behaviour of early age concrete, concrete without early age, aggregate cooled and pipe cooled concrete.

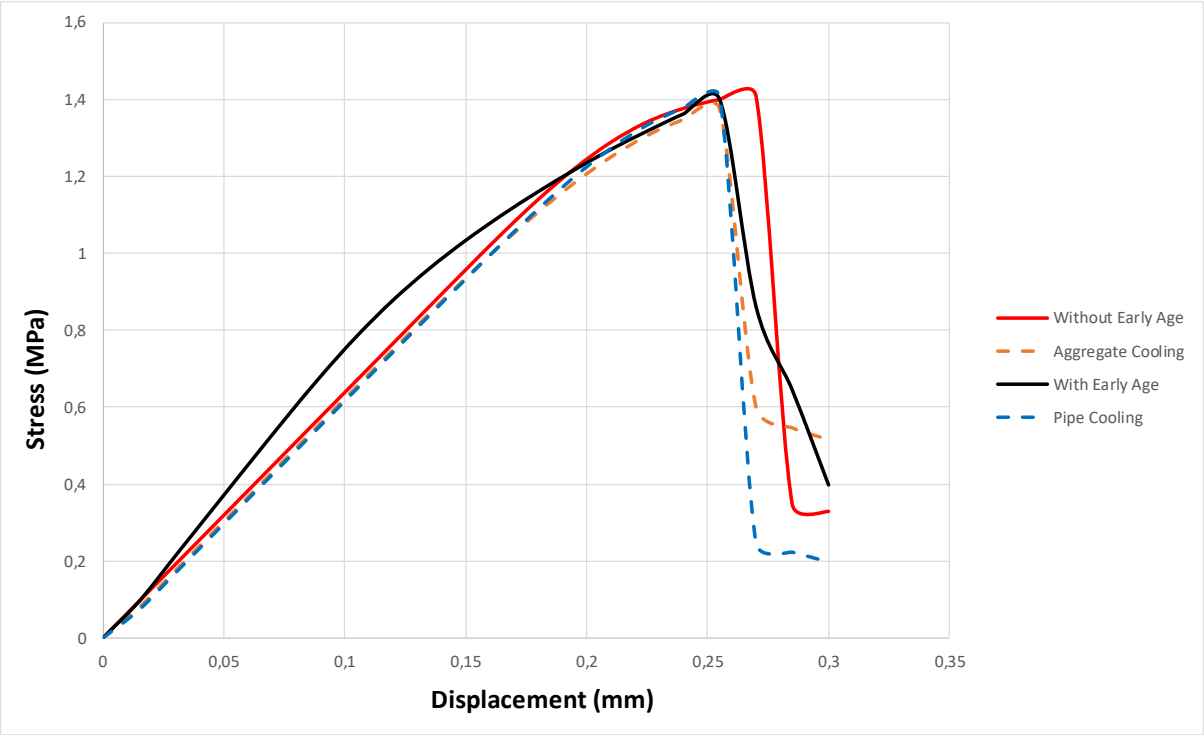

Figure 4-8 Global mechanical behaviour of aggregate, pipe cooled, EA concrete and WEA concrete under tension.

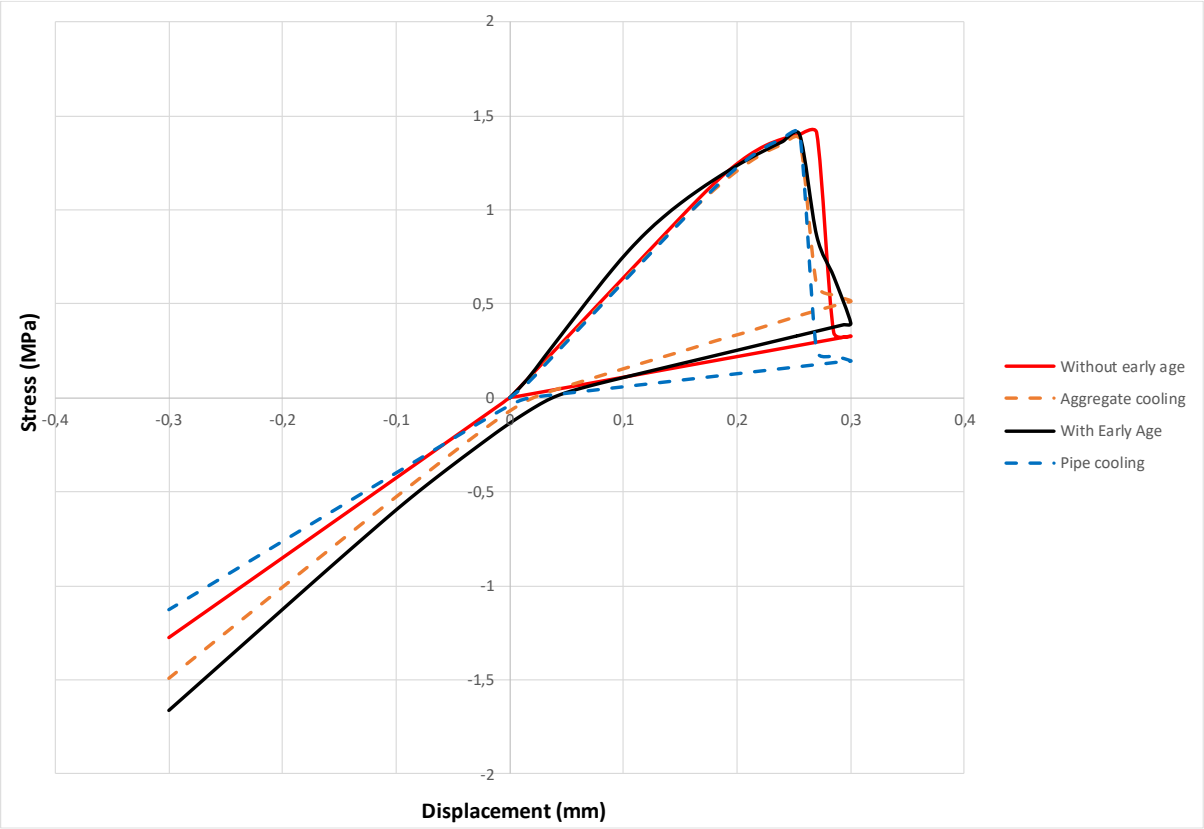

Figure 4-9 Global mechanical behaviour of aggregate, pipe cooled, EA concrete and WEA concrete under cyclic loading.

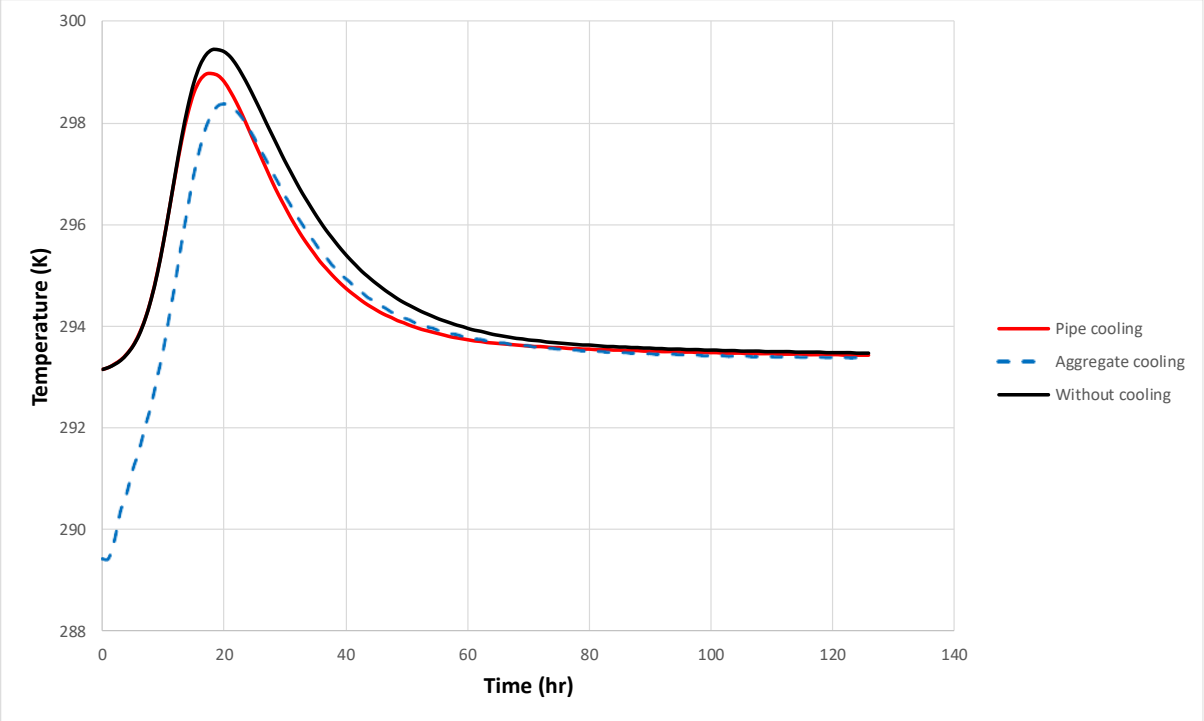

Figure 4-10 Temperature evolution of pipe cooling, aggregate cooling and early age without cooling.

On a global perspective, we observe a general decrease in the maximum hydration temperature reached by the concrete samples with either aggregate cooling or pipe cooling, see Figure 4-10. Adding on to that, there's a clear improvement on the seam reclosing stresses in the samples which were precooled, see Figure 4-9.

4.3.5 Effect of Different Cooled Aggregate Compositions on Early Age Concrete.

5/8; 8/ 16; 16/25 **5/7; 7/ 16; 16/21**

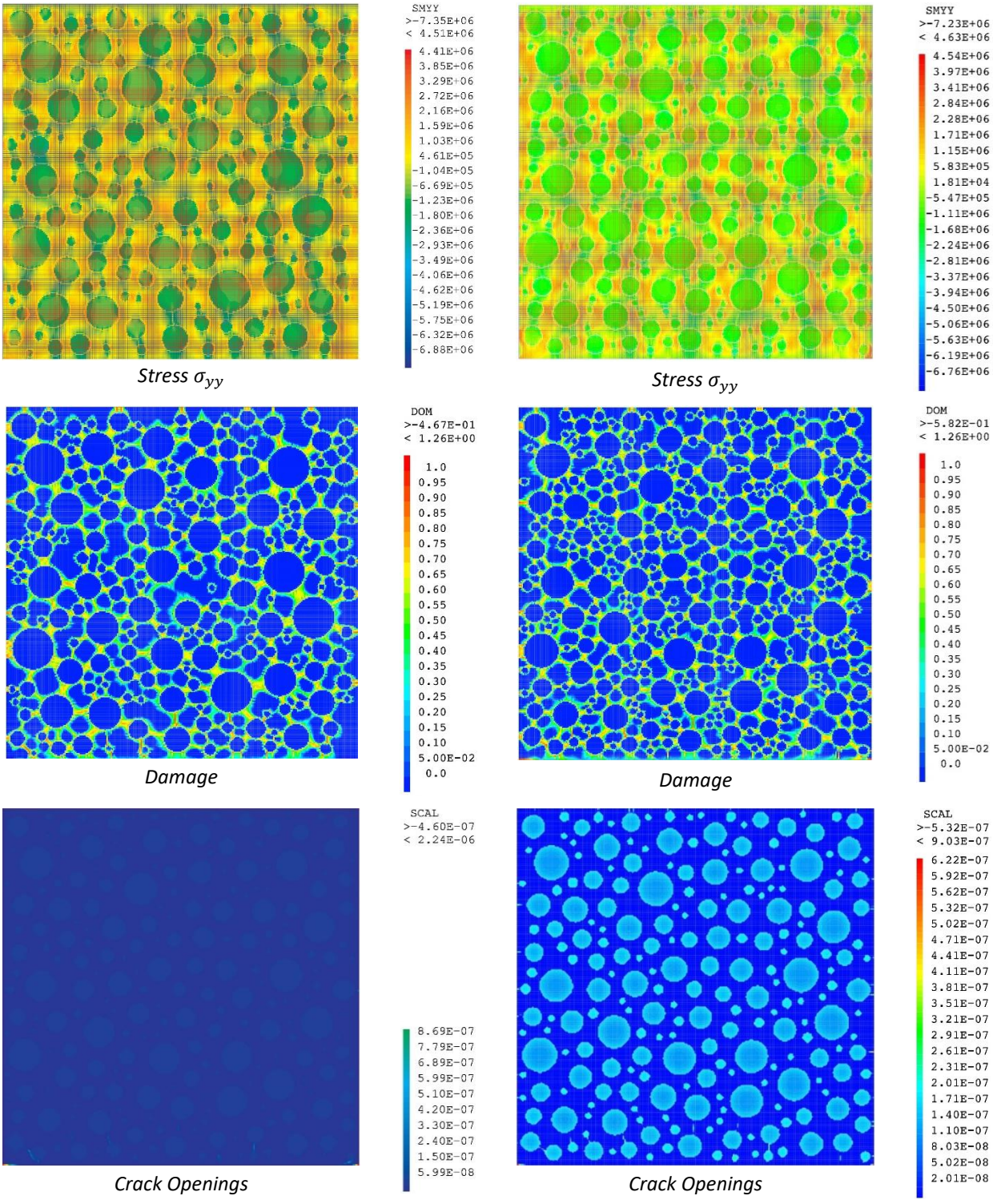

Stress σ_{yy} *Stress σ_{yy}*

Damage *Damage*

Crack Openings *Crack Openings*

Figure 4-11 Stress, damage and crack openings due to early age only.(Aggregate and pipe cooled)

4.3.5.1 Temperature evolution.

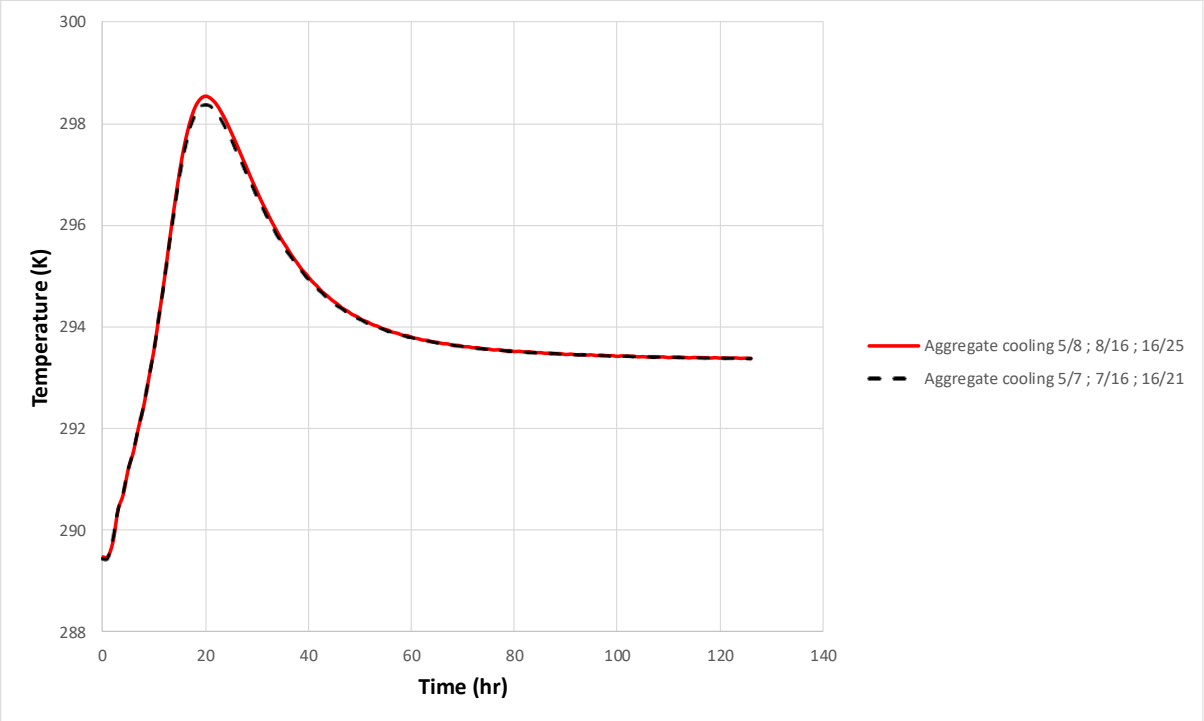

Figure 4-12 Hydration temperature evolution of aggregate cooled models with different granular classes.

Figure 4-11 shows a relatively comparable damage field and crack openings due to early age hydration only for the two samples with different aggregate compositions

Figure 4-12 shows the temperature evolution of the two samples with an almost identical evolution, although the sample with aggregate class composition of (5/8; 8/16; 16/25) reaches a slightly higher maximum hydration temperature. This qualifies the notion that different aggregates can influence the degree of impact of hydration in concrete.

4.3.6 Effect of Different Cooled Aggregate Compositions on Early Age Concrete under tension.

5/8; 8/ 16; 16/25 **5/7; 7/ 16; 16/21**

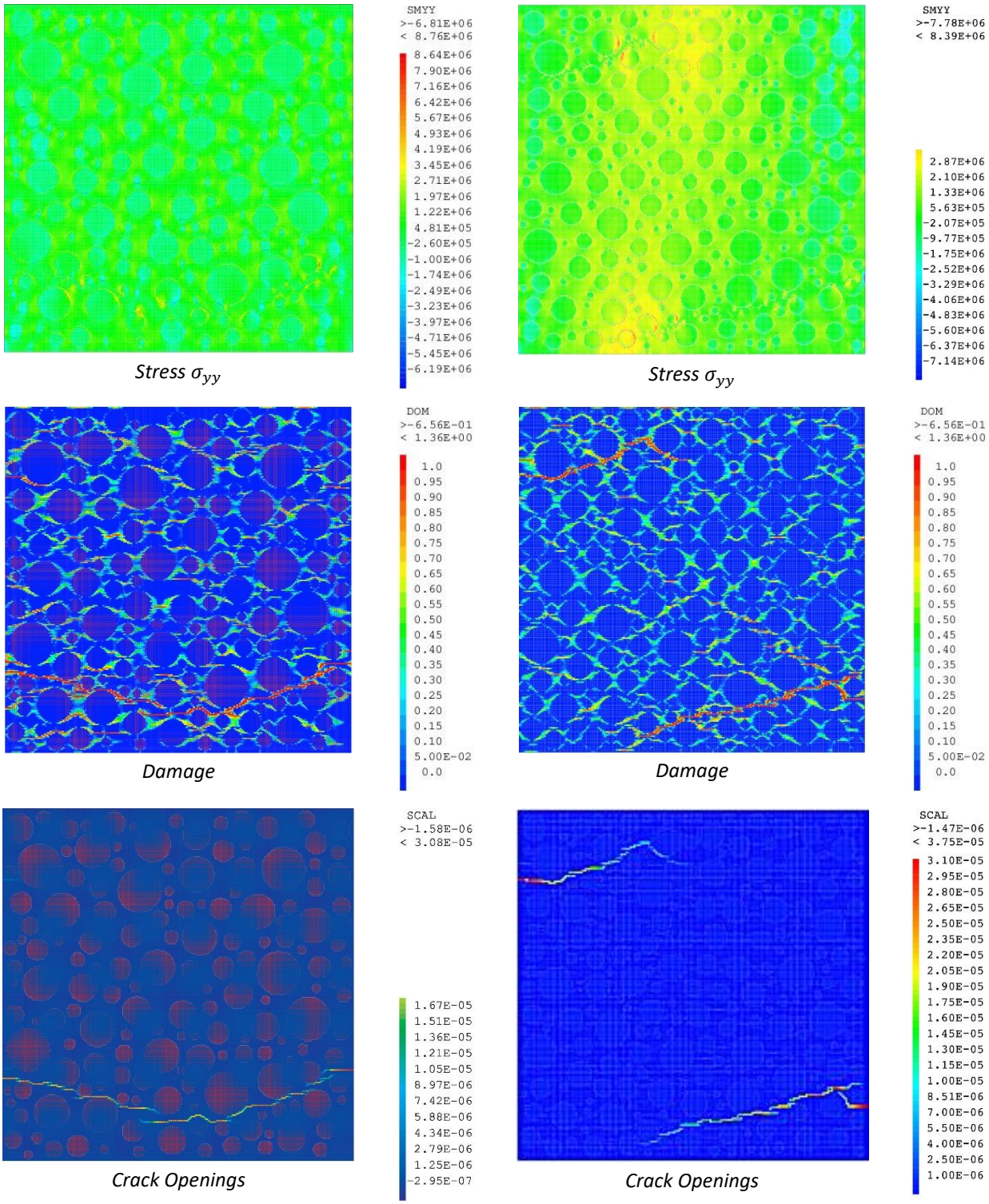

Stress σ_{yy} *Stress σ_{yy}*

Damage *Damage*

Crack Openings *Crack Openings*

Figure 4-13 Stress, damage and crack openings due to early age and under tension. (Aggregate and pipe cooled)

4.3.6.1 Global mechanical behaviour under tension.

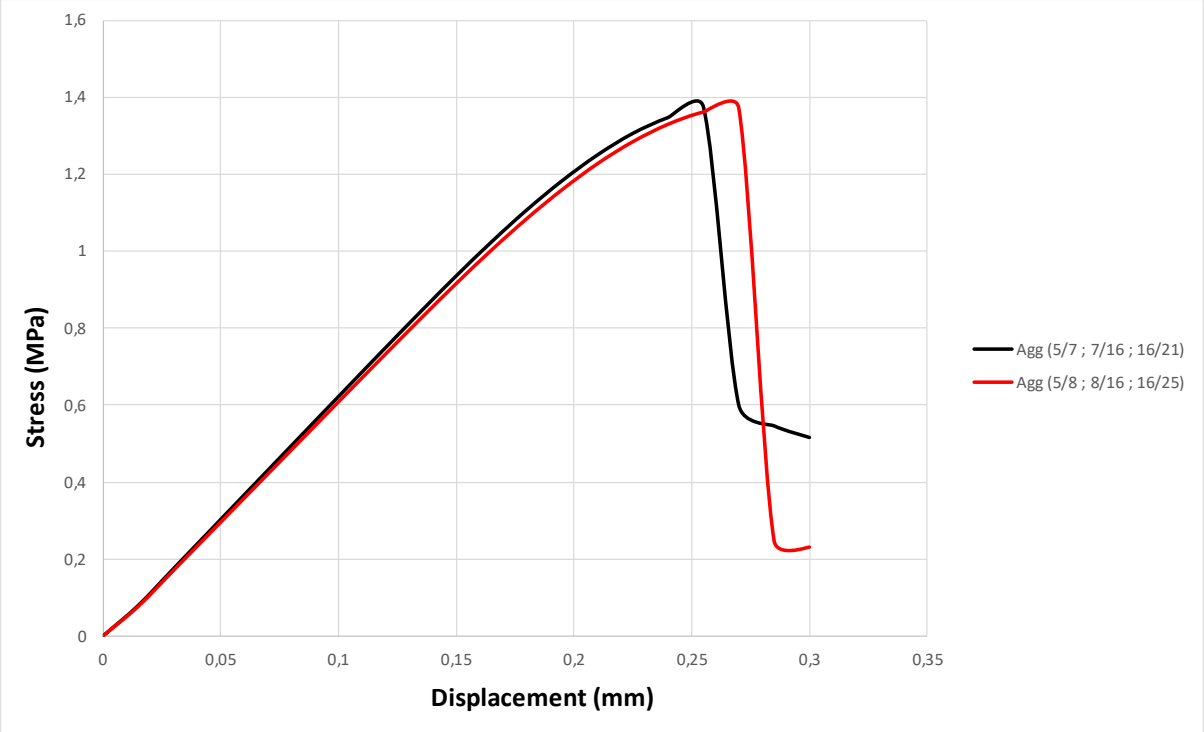

Figure 4-14 Global mechanical behaviour of concrete under tension loading. Effect of different granular classes.

In Figure 4-13 we see that Agg (5/7; 7/16; 16/21) has 2 primary seams as compared to one of Agg (5/8; 8/16; 16/25). This is consistent with illustrations of Figure 4-14 which depicts the mechanical behaviour of the two aggregate cooled samples. Agg (5/8; 8/16; 16/25) has a prolonged quasi elastic phase as compared to Agg (5/7; 7/16; 16/21).

4.3.7 Effect of Different Cooled Aggregate Compositions on Early Age Concrete subjected to cyclic loading.

5/8; 8/ 16; 16/25 **5/7; 7/ 16; 16/21**

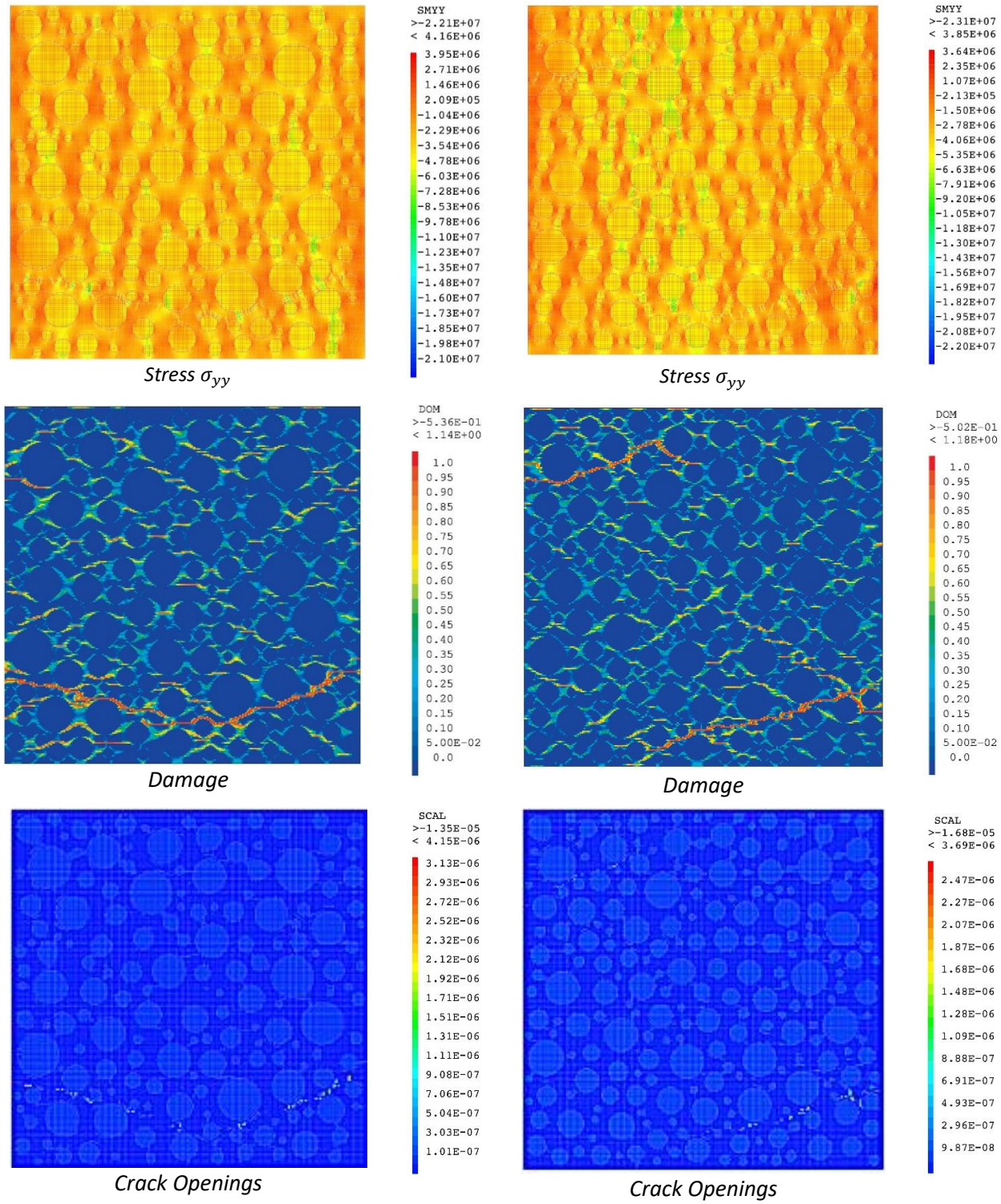

Figure 4-15 Stress, damage and crack openings due to early age under cyclic loading. (Aggregate and pipe cooled)

4.3.7.1 Global mechanical behaviour under cyclic loading.

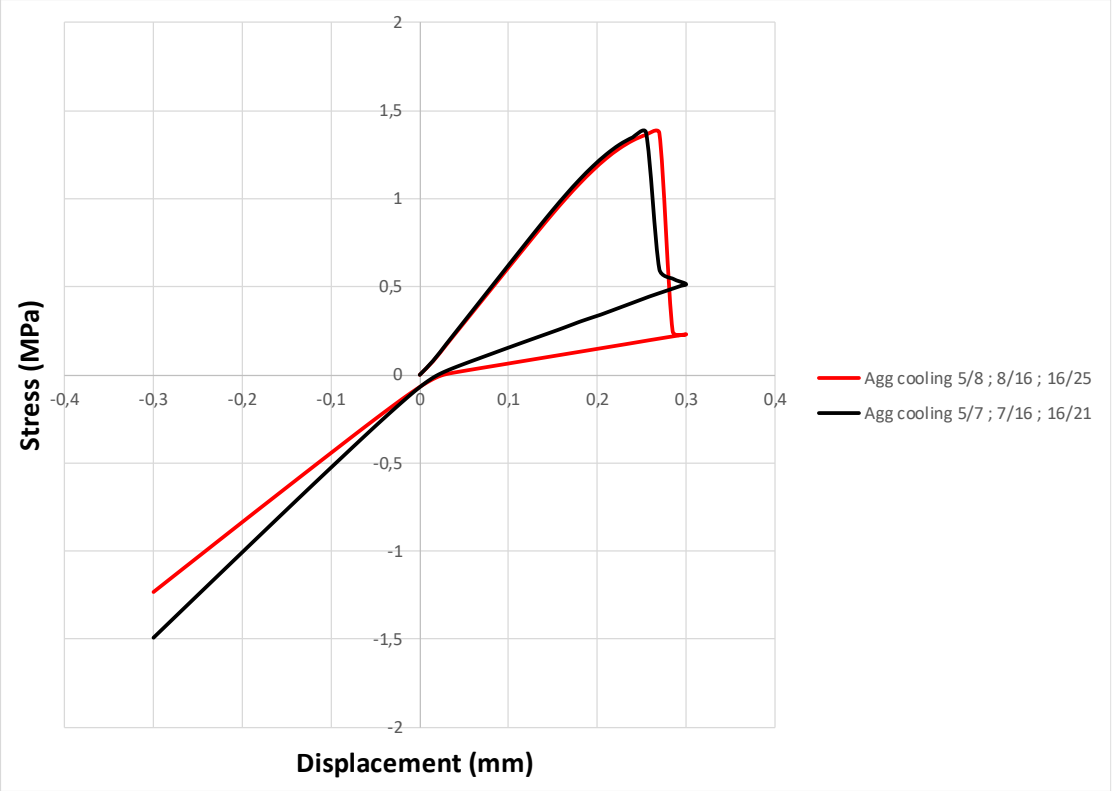

Figure 4-16 Global mechanical behaviour of concrete under cyclic loading. Effect of different granular classes.

Figure 4-16 Illustrates the mechanical behaviour of the two aggregate samples under cyclic loading. The seam reclosing stresses are almost identical although the positive and negative elastoplastic phases are different.

4.4 Conclusion.

The concrete numerical modelling carried out in this chapter demonstrated the effects of aggregate cooling and pipe cooling on the stress and temperature evolution of concrete under early age hydration. A marked temperature reduction was visible from both methods and significant mechanical recovery was also noted. A comparison between the two methods was undertaken, with aggregate cooling proving to be a more efficient method of hydration temperature reduction. Pipe cooling though, exhibits more favorable mechanical characteristics and an overall final behavior. It was also noted that different aggregate compositions can affect early age behavior of concrete.

General conclusion.

The objective of this master project was to discuss and analyse the early age behaviour of concrete in massive structures and give an insight on the various ways of reducing the impact of early age cracking in concrete. A brief explanation on the root cause of the early age problem in concrete was presented and its associated effects. The exothermic reaction of cement hydration results in various forms of shrinkage at early age namely autogenous, drying, thermal and chemical shrinkage. Bar shrinkage, early age hydration also causes creep in concrete which is also problematic in the long-term mechanical behaviour of a structure. The project went on to elaborate various methods of combating and limiting the early age effect of hydration in concrete. Of the existing pool of methods, two were used in simulations to quantify their impact on reducing early age damage in concrete structures due to hydration using a software called Cast3m. By the use of numerical simulations, it was established that early age hydration in concrete induces cracks in concrete. This is due to initial stresses developing because of steep temperature gradients produced by hydration exothermic reactions.

A qualitative numerical simulation was conducted to study the effect of dimensions on the maximum hydration temperature. The findings of the simulations affirmatively concluded that hydration temperature is influenced by the amount of concrete casted. Of the two cooling methods compared, findings showed that aggregate cooling had lower initial and maximum hydration temperature as compared to pipe cooling. Pipe cooling was also found to have a slightly less negative seam reclosing stress and therefore leading to less cracking. The two cooling methods were found to definitively reduce cracking in early age concrete. Lastly, a study on the effect of different aggregate cooled granular class compositions was carried out. Simulations showed a slight difference, with both samples exhibiting an almost identical hydration temperature evolution and the same seam reclosing stresses. This was due to minute differences in the types of granular class compositions used.

Recommendations.

Further study on the following themes can be pursued to enrich the study of this domain:

- Early age effect of concrete in massive structures under extreme conditions.
- Shrinkage and creep coupled with early age hydration for the prediction of concrete behaviour in massive structures.
- Application of concrete cooling methods in real massive structures.
- Numerical modelling of hydration induced fracture propagation in concrete.
- Response of massive structures due to early age cracking.

References

ACI. (1998). *Cooling and Insulating Systems for Mass Concrete* (ACI 207.4R-93, p. 22).

ACI. (2017). *Reduction of crack width with fiber*. https://www.concrete.org/Publications/InternationalConcreteAbstractsPortal.aspx?m=results&Publication=Special+Publication&volume=319

Arrhenius, S. (1916). Quantitative Laws in Biological Chemistry. *Nature*, *96*(2410), 508–508. https://doi.org/10.1038/096508a0

Briffaut, M. (2010). *Étude de la fissuration au jeune âge des structures massives en béton: Influence de la vitesse de refroidissement, des reprises de bétonnage et des armatures* [Thèse de Doctorat]. ECOLE NORMALE SUPERIEURE DE CACHAN.

Briffaut, M., Benboudjema, F., Torrenti, J. M., & Nahas, G. (2011). Numerical analysis of the thermal active restrained shrinkage ring test to study the early age behavior of massive concrete structures. *Engineering Structures*, *33*(4), 1390–1401. https://doi.org/10.1016/j.engstruct.2010.12.044

CEB-FIP (Ed.). (1993). *CEB-FIP model code 1990: Design code*. T. Telford.

Charpin, J., Myers, T., Fitt, A. D., Fowkes, N., Ballim, Y., & Patini, A. P. (2004). *PIPED WATER COOLING OF CONCRETE DAMS*. 17. https://core.ac.uk/search?q=repositories.id:(70).

Fichant, S., La Borderie, C., & Pijaudier-Cabot, G. (1999). Isotropic and anisotropic descriptions of damage in concrete structures. *MECHANICS OF COHESIVE-FRICTIONAL MATERIALS*, *4*, 21. https://hal.archives-ouvertes.fr/hal-01007002.

Gambali, A. K., & Shanagam, N. K. (2014). Creep of Concrete. *International Journal of Engineering Development and Research*, *2*(4). https://www.ijedr.org/papers/IJEDR1404068.pdf

Ghezali, S. (2012). *Modelisation Numerique de la fissuration des Structures en Beton Arme: Application a la Simulation des Enceintes de Confinement* [Memoire de Magistere]. Université de Tlemcen.

Hedlund, H., & Groth, P. (1998). Air cooling of concrete by means of embedded cooling pipes-Part I: Laboratory tests of heat transfer coefficients. *Materials and Structures*, *31*(5), 329–334. https://doi.org/10.1007/BF02480675

Hilaire, A. (2014). *Etude des déformations différées des bétons en compression et en traction, du jeune au long terme: Application aux enceintes de confinement* [Thèse de Doctorat, ÉCOLE NORMALE SUPÉRIEURE DE CACHAN]. https://tel.archives-ouvertes.fr/tel-01149230.

Holt, E. (2001). Early age autogenous shrinkage of concrete. *Technical Research Centre of Finland, VTT Publications 446*, 184.

Ile, N. (2000). *CONTRIBUTION A LA COMPREHENSION DU FONCTIONNEMENT DES VOILES EN BETON ARME SOUS SOLLICITATION SISMIQUE: APPORT DE L'EXPERIMENTATION ET DE LA MODELISATION A LA CONCEPTION* [These de Doctorat, L'INSTITUT NATIONAL

DES SCIENCES APPLIQUEES DE LYON]. https://www.researchgate.net/profile/Ile-Nicolas/publication/37813204

Illston, J. M., & Sanders, P. D. (1973). The effect of temperature change upon the creep of mortar under torsional loading. *Magazine of Concrete Research*, *25*(84), 136–144. https://doi.org/10.1680/macr.1973.25.84.136

Iowa DOT. (n.d.). *Early-Age Cracking (temperature, shrinkage, strength)*. National Concrete Pavement Technology Center Iowa's Lunch–Hour Workshop In cooperation with the Iowa DOT and the Iowa Concrete Paving Association. https://intrans.iastate.edu/app/uploads/sites/7/2019/08/36_Early-Age-Cracking-Troubleshooting.pdf

Jensen, O. M. (2005). *Autogenous phenomena in cement-based materials*. Department of Civil Engineering, Aalborg University.

Jensen, O. M., Hansen, P. F., Lachowski, E. E., & Glasser, F. P. (1999). Clinker mineral hydration at reduced relative humidities. *Cement and Concrete Research*, *29*(9), 1505–1512. https://doi.org/10.1016/S0008-8846(99)00132-5

Justnes, H., Van Gemert, A., Verboven, F., & Sellevold, E. J. (1996). Total and external chemical shrinkage of low w/c ratio cement pastes. *Advances in Cement Research*, *8*(31), 121–126. https://doi.org/10.1680/adcr.1996.8.31.121

Kachanov, L. M. (1986). *Introduction to continuum damage mechanics*.

Kaium, A. S. (n.d.). *Estimation of the heat evolutionduring the hydration of concrete,mix design of hot concrete, dryingand coatingof concrete structures*. Aalto. https://mycourses.aalto.fi/pluginfile.php/130851/mod_label/intro/2015-10-23_heat_evolution_Fahim01.pdf

Kell, G. S. (1975). Density, Thermal Expansivity, and Compressibility of Liquid Water from 0" to 150°C: Correlations and Tables for Atmospheric Pressure and Saturation Reviewed and Expressed on 1968 Temperature Scale. *Journal of Chemical and Engineering Data*, *20*(1), 9.

Klemczak, B., & Knoppik-Wróbel, A. (2011). EARLY AGE THERMAL AND SHRINKAGE CRACKS IN CONCRETE STRUCTURES – DESCRIPTION OF THE PROBLEM. *Architecture Civil Engineering Environment*, *2*(1), 15.

La Borderie, C., Matallah, M., NGuyen, T. D., Briffaut, M., & Benboud, F. (2010). *Hydration induced meso-stresses in concrete and their con- sequences on the cyclic behavior*.

Lagundžija, S., & Thiam, M. (2017). *Temperature reduction during concrete hydration in massive structures* [Master's thesis]. KTH, Royal Institute of Technology.

Lermitte, J. (2010). *Benchmark SMART 2008, phase 1, Synthetics results report* (p. 148). Département de modélisation des systèmes et structures, Service d'études mécaniques et thermiques.

Liseikin, A. V., Seleznev, V. S., & Adilov, Z. A. (2019). Determining the Natural Frequencies and Modes of Vibration of the Chirkey Arch Dam by the Standing-Wave Method. *Power Technology and Engineering*, *53*(1), 39–43. https://doi.org/10.1007/s10749-019-01031-x

Lu, Y. (2013). Modelling the dynamic response of concrete with mesoscopic heterogeneity. In *Understanding the Tensile Properties of Concrete* (pp. 218–272e). Elsevier. https://doi.org/10.1533/9780857097538.2.218

Matallah, M., La Borderie, C., & Maurel, O. (2009). A practical method to estimate crack openings in concrete structures. *International Journal for Numerical and Analytical Methods in Geomechanics*, 18. https://doi.org/10.1002/nag.876

Mazars, J. (1984). *APPLICATION DE LA MECANIQUE DE L'ENDOMMAGEMENT AU COMPORTEMENT NON LINEAIRE ET A LA RUPTURE DU BETON DE STRUCTURE*. Éditeur inconnu. https://books.google.dz/books?id=Dxa4OwAACAAJ

Mills, R. H. (1966). *Factors Influencing Cessation of Hydration in Water Cured Cement Pastes*. Department of Civil Engineering, University of the Witwatersrand.

Muguti, E., Kulemeka, N., & Ndinya, E. (2015). *KARIBA DAM REHABILITATION PROJECT* (P-Z1-FA0-075; p. 24). African Development Bank Group. Multinational_-_Kariba_Dam_Rehabilitation_Project_-__ESIA_Summary_-_11_2015.pdf

Neville, A. M., & Brooks, J. J. (2010). *Concrete technology* (2. ed). Prentice Hall.

Neville, A. M., Dilger, W. H., & Brooks, J. J. (1983). *Creep of plain and structural concrete*. Construction Press.

NGuyen, T. D. (2010). *Apport de la modélisation mésoscopique dans la prédiction des écoulements dans les ouvrages en béton fissuré en conditions d'accident grave* [Thèse de Doctorat]. Université de Pau et des Pays de l'Adour.

Nguyen, T.-T., Waldmann, D., & Bui, T. Q. (2019). Computational chemo-thermo-mechanical coupling phase-field model for complex fracture induced by early-age shrinkage and hydration heat in cement-based materials. *Computer Methods in Applied Mechanics and Engineering*, *348*, 1–28. https://doi.org/10.1016/j.cma.2019.01.012

Online Civil Engineering. (n.d.). *Creep of Concrete*. http://civil-online2010.blogspot.com/2015/02/creep-of-concrete.html

Powers, T., & Brownyard, T. L. (1946). Studies of the Physical Properties of Hardened Portland Cement Paste. *ACI Journal Proceedings*, *43*(9). https://doi.org/10.14359/15302

Qian, C., & Gao, G. (2012). Reduction of interior temperature of mass concrete using suspension of phase change materials as cooling fluid. *Construction and Building Materials*, *26*(1), 527–531. https://doi.org/10.1016/j.conbuildmat.2011.06.053

Safiuddin, Md., Kaish, A., Woon, C.-O., & Raman, S. (2018). Early-Age Cracking in Concrete: Causes, Consequences, Remedial Measures, and Recommendations. *Applied Sciences*, *8*(10), 1730. https://doi.org/10.3390/app8101730

Sellevold, E. J., & Bjøntegaard, Ø. (2006). Coefficient of thermal expansion of cement paste and concrete: Mechanisms of moisture interaction. *Materials and Structures*, *39*(9), 809–815. https://doi.org/10.1617/s11527-006-9086-z

Shitov, S. P., Gunter, Yu. S., & Kraitser, A. L. (1976). Cooling the concrete aggregates used for construction of the Chirkey hydroelectric plant. *Hydrotechnical Construction*, *10*(3), 257–263. https://doi.org/10.1007/BF02407372

Slowik, V., Hübner, T., Schmidt, M., & Villmann, B. (2009). Simulation of capillary shrinkage cracking in cement-like materials. *Cement and Concrete Composites*, *31*(7), 461–469. https://doi.org/10.1016/j.cemconcomp.2009.05.004

Taylor, J. (2020). *Food security and food sovereignty in the Creston Valley of British Columbia*. https://doi.org/10.14288/1.0390002

Ullah, F. (2017). *Early Age Autogenous Shrinkage and Long-term Drying Shrinkage of Fibre Reinforced Concrete.* [Master's thesis]. Aalto University.

Ulm, F.-J., & Coussy, O. (1995). Modeling of Thermochemomechanical Couplings of Concrete at Early Ages. *Journal of Engineering Mechanics*, *121*(7), 785–794. https://doi.org/10.1061/(ASCE)0733-9399(1995)121:7(785)

Waller, V. (1999). *Relations entre composition des betons, exothermie en cours de prise et resistance en compression* [Thèse de Doctorat, École Nationale des Ponts et Chaussées]. https://hal-enpc.archives-ouvertes.fr/tel-01223803.

Wittmann, F. H., Beltzung, F., & Zhao, T. J. (2009). Shrinkage mechanisms, crack formation and service life of reinforced concrete structures. *International Journal of Structural Engineering*, *1*(1), 13. https://doi.org/10.1504/IJSTRUCTE.2009.030023

Zheng, Z., & Wei, X. (2021). Mesoscopic models and numerical simulations of the temperature field and hydration degree in early-age concrete. *Construction and Building Materials*, *266*, 121001. https://doi.org/10.1016/j.conbuildmat.2020.121001

Zreiki, J. (2009). *Comportement du béton au jeune âge dans les structures massives. Application au cas de réparation des ouvrages.* [Thèse de Doctorat, École normale supérieure de Cachan]. https://tel.archives-ouvertes.fr/tel-00466966.